SIAM J. Applied Dynamical Systems
Vol. 18, No. 1, pp. 418–457

Comparison of Combinatorial Signatures of Global Network Dynamics Generated by Two Classes of ODE Models*

Peter Crawford-Kahrl†, Bree Cummins†, and Tomas Gedeon†

Abstract. Modeling the dynamics of biological networks introduces many challenges, among them the lack of first principle models, the size of the networks, and difficulties with parameterization. Discrete time Boolean networks and related continuous time switching systems provide a computationally accessible way to translate the structure of the network to predictions about the dynamics. Recent work has shown that the parameterized dynamics of switching systems can be captured by a combinatorial object, called a Dynamic Signatures Generated by Regulatory Networks (DSGRN) database, that consists of a parameter graph characterizing a finite parameter space decomposition, whose nodes are assigned a Morse graph that captures global dynamics for all corresponding parameters. We show that for a given network there is a way to associate the same type of object by considering a continuous time ODE system with a continuous right-hand side, which we call an L-system. The main goal of this paper is to compare the two DSGRN databases for the same network. Since the L-systems can be thought of as perturbations (not necessarily small) of the switching systems, our results address the correspondence between global parameterized dynamics of switching systems and their perturbations. We show that, at corresponding parameters, there is an order preserving map from the Morse graph of the switching system to that of the L-system that is surjective on the set of attractors and bijective on the set of fixed-point attractors. We provide important examples showing why this correspondence cannot be strengthened.

Key words. switching system, regulatory network, Boolean network, Morse graph, combinatorial dynamics

AMS subject classification. 37N25

DOI. 10.1137/18M1163610

1. Introduction.

In problems arising in cellular biology, there is a need to model many mutually interacting types of molecules that together control cellular fate. Incorrectly functioning genetic and regulatory networks are at the core of cancer, diabetes, and other systemic diseases [11, 13, 31]. Because of the crucial importance of these networks for cell biology and human health, the development of effective methods that can characterize the dynamics supported by a network over all parameters is a high priority [2, 4, 27, 3, 29, 30, 32]. In the

*Received by the editors January 2, 2018; accepted for publication (in revised form) by K. Josic January 8, 2019; published electronically February 28, 2019.

http://www.siam.org/journals/siads/18-1/M116361.html

Funding: The work of the first author was supported by USP and INBRE student research grants at Montana State University. The work of the second and third authors was partially supported by grants USDA 2015-51106-23970, DARPA grants D12AP200025 and FA8750-17-C-0054, and NIH 1R01GM126555-01. The work of the third author was also partially supported by NSF grants DMS-1226213, DMS-1361240, and NIH grant 1R01AG040020-01. Research reported in this publication was supported by the National Institute of General Medical Sciences of the National Institutes of Health under Award P20GM103474. The content is solely the responsibility of the authors and does not necessarily represent the official views of the National Institutes of Health.

†Mathematical Sciences, Montana State University, Bozeman, MT 59717 (peter.crawfordkahrl@student.montana.edu, cummins@math.montana.edu, gedeon@math.montana.edu).

context of cell biology, the problems of nonlinear dynamics are compounded by the lack of first principles that would determine appropriate nonlinearities, the difficulty in obtaining precise experimental data needed to determine parameters, and the need to analyze the dynamics of 5–10 dimensional systems over 30–50 parameters.

Recently, we introduced in [16, 15] a new approach to this problem that assigns two finite objects to any network with positive and negative edges. First is a *parameter graph* whose nodes are in 1-1 correspondence with regions in the parameter space, where these regions form a decomposition of the parameter space. To each region of the parameter space, i.e., a node of the parameter graph, there is an associated *state transition graph* that characterizes allowable transitions between well-defined states that partition the phase space. Since state transition graphs can be large, a useful description of the recurrent trajectories is a *Morse graph*, which is the graph of strongly connected path components of the state transition graph. This information is compiled into a database of Dynamic Signatures Generated by Regulatory Networks (DSGRN database), where to each node of the parameter graph there is an associated Morse graph that captures the recurrent dynamics valid for all parameters in the corresponding parameter region.

The advantages of such a description of global dynamics is its finiteness and the resulting computability; yet this description, which inevitably must be coarser than the traditional concepts of dynamical systems theory, allows searching the database for parameters that support dynamics like bistability, hysteresis, nonconstant recurrent behavior, and enables the comparison of the prevalence of such signatures across multiple networks. There have been applications of formal model checking to state transition graphs [20] answering questions about steady states and their reachability from a given initial state, even for parameterized systems.

The development of DSGRN was guided by work over the last two decades on *switching systems* [24, 35, 36, 9, 17, 18] which are ordinary differential equations with piecewise constant nonlinearities. The value of each nonlinearity changes discontinuously when an argument crosses a threshold. The collection of these thresholds divides the phase space into domains, which form the states (nodes) of the state transition graph.

The relationship between a combinatorial description of the dynamics and a much finer description in terms of a compatible ODE system is a very interesting problem. One approach to the formalization of the relationship between models on different levels of abstraction has been proposed in [14, 10], and applied to cell biology models in [1]. There has been a considerable interest in the computational biological systems community in trying to enlarge a class of ODE systems for which finite state transition graphs capture the behavior of all solutions [5, 6, 7, 8]. The result of these papers show how to construct a state transition graph for so called multiaffine systems, where nonlinearities are piecewise linear functions.

We introduce a general framework for the construction of state transition graphs. This framework encompasses the well-known case of Boolean maps [34, 35, 36, 12, 33], and extends it to a *multilevel discrete map* D, which increases the number of discrete states available to each node in the network [21, 25]. We then introduce the idea of a *nearest neighbor multivalued map* $\mathcal{F}$, which may arise as an *asynchronous update rule* of D in a way analogous to that discussed in [12] for a Boolean model. $\mathcal{F}$ obeys an adjacency condition which allows only one node of the network to change its state at a time. Each such map $\mathcal{F}$ is uniquely associated with a state transition graph.

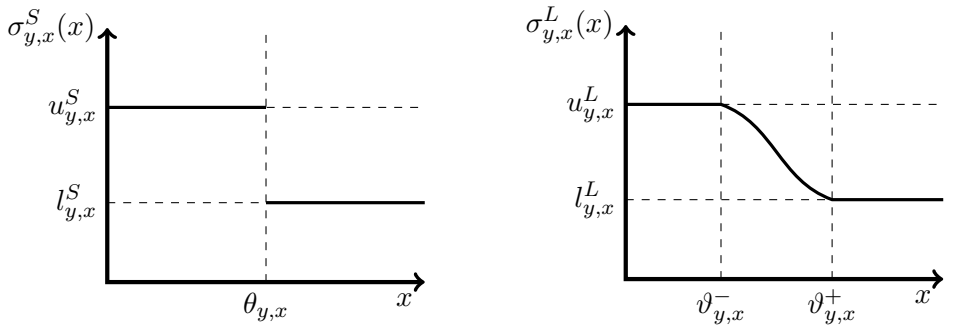

Figure 1. *(Left) A typical nonlinearity of the class of S-systems; (Right) a typical nonlinearity of the class of L-systems. The continuous transition must be bounded by the constant values on either side, but is not required to be monotone.*

We offer two examples of ordinary differential equation models associated with a regulatory network that are compatible with a nearest neighbor map $\mathcal{F}$, which we call S-systems and L-systems. While the S-systems, known as a switching system in the literature (see, e.g., [16, 19, 28]), have been very well studied, the L-systems admit nonlinearities that are step functions with Lipschitz continuous bridges, which we call L-functions. These functions have alternating intervals where the function is constant, and the intervals where the function is Lipschitz and bounded between the (constant) values of the function on neighboring intervals; see Figure 1. Importantly, the intervals where the L-functions are nonconstant are not required to be small.

In both S- and L-systems, the association between the continuous ODE system and a discrete map $\mathcal{F}$ allows us to combine the best features of both worlds. On one hand, there is a combinatorial representation of both the dynamics and the parameters, which allows computational enumeration of all types of dynamics for all parameters. On the other hand, the underlying assumptions of continuity allow us to interpret the dynamics of iterates of $\mathcal{F}$ in terms of solutions of ODEs.

The central question that we address in this paper is the comparison of the global dynamics of S- and L-systems of ODEs for a given regulatory network, as captured by the state transition graphs associated with the maps $\mathcal{F}^S$ and $\mathcal{F}^L$. This investigation is a global version of a question that has been explored before where a piecewise constant nonlinearity is perturbed around a threshold to form a continuous function [17, 28, 22]. In this paper we address this question by comparing the Morse graphs associated with $\mathcal{F}^L$ and $\mathcal{F}^S$.

Our main results include (1) the existence of an inclusion map between collections of parameter regions of S- and L-systems for the same network that (2) induces an order-preserving map on corresponding Morse graphs associated with these parameter regions. Furthermore, this map is (3) a bijection on Morse nodes that correspond to stable fixed points of the corresponding ODEs, and (4) a surjection on the attracting Morse nodes of the Morse graphs. We conclude with a series of examples that demonstrate that these relationships cannot be strengthened.

To aid the reader in following the exposition of the manuscript, we have included a table of important notation, Table 1, which is centrally located for easy reference.

Table 1
Table of notation.

$\mathbf{RN}$	a regulatory network	Def. 2.1
$\mathbf{T}(i)$, $\mathbf{S}(i)$	targets, sources of a node i	Def. 2.1
$I_{k,i}$	interval of semiaxis $[0,\infty)$ of x_i	sect. 2
$\mathcal{K}$	the collection of domains in $[0,\infty)^N$	sect. 2
$\mathcal{V}$, $\mathcal{V}^*$	collection of all states (for a $*$-system)	Def. 2.2, 3.6, 3.12
g, g^*	map relating domains $\mathcal{K}$, $\mathcal{K}^*$ to states $\mathcal{V}$, $\mathcal{V}^*$	Def. 2.2
G, G^*	state function from $[0,\infty)^N$ to $\mathcal{V}$, $\mathcal{V}^*$ (for a $*$-system)	Def. 2.2
Ξ	collection of transmitted values	Def. 2.2
F	transmission function from $\mathcal{V}$ to Ξ	Def. 2.2
M	map from transmitted values Ξ to output value $[0,\infty)^N$	Def. 2.2
D	multilevel discrete map $G \circ M \circ F$	Def. 2.2
$\mathcal{F}$, $\mathcal{F}^*$	nearest neighbor multivalued map (for a $*$-system)	Def 2.4, 3.6, 3.12
$(\mathcal{V},\mathcal{E})$, $(\mathcal{V}^*,\mathcal{E}^*)$	state transition graph (for a $*$-system)	Def. 2.4, sect. 3.1, 3.2
$\mathcal{M}$, MD, MG	a Morse set, Morse decomposition, and Morse graph	Def. 2.5, 2.6
γ_i^*	decay rate of x_i in $*$-system	sect. 2.1, 2.2
$\theta_{j,i}$	threshold of edge (i,j) in S-system	sect. 2.1
$\vartheta_{j,i}^{\pm}$	thresholds of edge (i,j) in L-system	sect. 2.2
$l_{j,i}^*$, $u_{j,i}^*$	low and high values of edge (i,j) in *-system	sect. 2.1, 2.2
σ^*	regulatory function, piecewise constant, or Lipschitz bridge	sect. 2.1, 2.2
Λ^*	combination of σ^* describing $\dot{x}$ (for a $*$-system)	eqs. (7), (10)
z^*	$*$-parameter, $z^S=(l^S,u^S,\theta,\gamma^S)$, $z^L=(l^L,u^L,\vartheta^-,\vartheta^+,\gamma^L)$	sect. 2.1, 2.2
Z^*	collection of regular $*$-parameters	Def. 3.4
φ	threshold in either system	Def. 3.1
ζ	cell in phase space	Def. 3.1
$ND(\zeta)$	nondegenerate intervals of ζ	Def. 3.1
κ	a domain (N-dimensional cell ζ)	Def 3.1, sect. 2
$\mathcal{K}^*$	collection of domains in $*$-system	Def. 3.1
$\mathcal{K}_N^L$	domains with all σ constant	Def. 3.1
$\mathcal{K}_{N-1}^L$	domains with exactly one σ not constant	Def. 3.1
$\tau_j^{\pm}$	face of a domain, either left ($-$) or right ($+$)	Def. 3.2
(τ,κ)	wall of a domain	Def. 3.2
$\mathcal{W}(z)$	collection of walls for parameter z	Def. 3.2
$\mathscr{L}^*$	wall labeling in $*$-system	Def. 3.5, 3.11
$\mathcal{C}(\zeta)$	set of corner points of a cell ζ	Def. 3.9
O	$\{O_i\}$, collection of orders	Def. 4.1
Ψ	includes $\mathcal{V}^S$ into $\mathcal{V}^L$	eq. (12)
$\overset{*}{\sim}$	equivalence relation on parameters in $*$-system	Def. 4.3
$\mathcal{Z}^*$	equivalence classes of parameters in $*$-system	Def. 4.3
Ω	canonical map from $\mathcal{Z}^S$ to $\mathcal{Z}^L$	Def. 4.5
ϕ	order-preserving map from MD^S to MD^L	Thm. 5.3
$\mathcal{A}^*$, A	$\mathcal{A}^*=\{A\}$ is the set of all attractors A in a $*$-system	Def. 5.4
FP	set of all fixed points	Def 5.6

* Refers to both S and L.

2. General system.

Definition 2.1. *A* regulatory network $\mathbf{RN}=(V,E)$ *is a directed graph with network nodes* $V=\{1,2,\ldots,N\}$ *and signed, directed edges* $E\subset V\times V\times\{\rightarrow,\dashv\}$. *For* $i,j\in V$, *we will use the notation* $(i,j)\in E$ *to denote a directed edge from* i *to* j *of either sign,* $i\rightarrow j$ *to denote an* activation *or positive interaction, and* $i\dashv j$ *to denote a* repression *or negative interaction.*

Figure 2. *Two dimensional example* ***RN****.*

We only consider regulatory networks with no negative self-regulation, $i \dashv i$. We exclude these networks because they present technical difficulties in switching systems; see [19] for an excellent set of references. In many cases, negative self-regulation can be replaced in a model by an intermediate node [19, 26] which obviates the need for a negative self-edge in a regulatory network.

We define the *targets* of a node i as

$$\mathbf{T}(i) := \{j \mid (i,j) \in E\}$$

and the *sources* of a node i as

$$\mathbf{S}(i) := \{j \mid (j,i) \in E\}.$$

We will occasionally use a simplified way to describe a network, where only the edges E are explicitly stated. As an example, we consider regulatory network $\mathbf{RN}$ given by $\{x \dashv y, y \dashv x\}$. Here the network has two nodes, x and y; see Figure 2.

One way to associate dynamics with a network is to construct a Boolean net [34, 35, 36, 12, 33]. Each node can attain values 0 or 1 that are interpreted as low and high levels of activity. At each node i with $|\mathbf{S}(i)| = n$, there is an associated local Boolean function that assigns to each of the 2^n input binary sequences a value of $x_i \in \{0,1\}$. The collection of the local Boolean functions over the network forms a Boolean function $B : \{0,1\}^N \to \{0,1\}^N$, that acts on a space of binary sequences of length N. Iterations B^r of this function model long-term behavior of the network. The collection of all local Boolean functions that can be selected at each node parameterizes the set of all Boolean functions $\mathcal{B}_{\mathbf{RN}}$ compatible with the given network $\mathbf{RN}$. Since both the domain $\{0,1\}^N$ of B and the parameterization of $\mathcal{B}_{\mathbf{RN}}$ are discrete sets, there is no concept of a "small" perturbation within the class $\mathcal{B}_{\mathbf{RN}}$.

Motivated by this example, we now propose a different way to associate a finite state dynamical system with a network. These dynamical systems will be parameterized by a continuous parameter space, and so it will make sense to ask how these finite dynamical systems behave under perturbations. Even though parameter space is continuous, we will show that it can be divided into a finite number of regions where a finite representation of the long-term dynamical behavior is fixed across a region, enabling a global description of the network over all real-valued parameters.

We start by assuming that with each node of the network there is an associated variable $x_i \in [0,\infty)$, which represents the concentration of chemical species i. We assume that there are a finite number of thresholds $\theta_{1,i}, \ldots, \theta_{m_i,i}$ that divide the semiaxis $[0,\infty)$ to $m_i + 1$ closed intervals $I_{k,i}$, where the subscript k denotes the ordering of the intervals on the real line. The effect of node i on its target nodes $j \in \mathbf{T}(i)$ will only depend on the interval $I_{k,i}$ and not on the particular value $x_i \in I_{k,i}$. The collection of thresholds $\{\theta_{j,i}\}$ partitions $[0,\infty)^N$ into a

finite number of domains: $\mathcal{K} = \{\prod_{i=1}^{N} I_{k,i}\}$, where we use the terminology $\kappa \in \mathcal{K}$ to denote a single domain. We let $x = (x_1, \ldots, x_N)$ denote a point in $[0, \infty)^N$.

Definition 2.2. *Let* $\mathcal{V}(i) := \{0, \ldots, m_i\}$ *and let*

$$G_i : [0, \infty) \to \mathcal{V}(i) \tag{1}$$

be a state function *defined by* $G_i(x_i) = k$ *if and only if* $x_i \in I_{k,i}$. *Let* $\mathcal{V} = \prod_i \mathcal{V}(i)$ *be the set of all* states *of the network* ***RN*** *and let*

$$G : [0, \infty)^N \to \mathcal{V}$$

be the vector-valued function with coordinate functions G_i. *For a given domain* κ, *the value* $G(x)$ *does not depend on* $x \in \kappa$ *and therefore we can assign the* state $s := G(x) \in \mathcal{V}, x \in \kappa$, *to the domain* κ, *which we will write as* $s := g(\kappa)$. *Viewed as a map on the set of domains* $\mathcal{K} = \{\kappa\}$ *in* $[0, \infty)^N$, g *is a bijection between domains* κ *and states* $s \in \mathcal{V}$,

$$g : \mathcal{K} \longrightarrow \mathcal{V}. \tag{2}$$

We postulate that along each edge (i, j) *in the network a signal from the node* i *to the node* j *can be transmitted, and this signal attains only a finite number of values* $\Xi_{j,i} := \{\xi_{j,i}^1 < \cdots < \xi_{j,i}^t\}$. *This transmission is characterized via a function*

$$F_{j,i} : \mathcal{V}(i) \to \Xi_{j,i} \tag{3}$$

that only depends on the state in $\mathcal{V}(i)$. *Let* $\Xi := \prod \Xi_{j,i}$ *be a product of all sets* $\Xi_{j,i}$ *and let*

$$F : \mathcal{V} \to \Xi$$

be the vector-valued function with coordinate functions $F_{j,i}$. *We define* F *in more detail in section* 2.1.

A final piece of our description of discrete dynamics on a network ***RN*** *is a collection of functions* M_i, *one for each node* i *of the network,*

$$M_i : \prod_{j \in \mathbf{S}(i)} \Xi_{i,j} \to [0, \infty), \tag{4}$$

that take the values that are being transmitted along the edges leading into i *and produce the values* x_i. *Let* M *be the vector-valued function with coordinate functions* M_i,

$$M : \Xi \to [0, \infty)^N,$$

and call it the combination function. *The composition*

$$D := G \circ M \circ F : \mathcal{V} \to \mathcal{V} \tag{5}$$

is a generalization of the Boolean function B, *called a* multilevel discrete function [21, 25]. *See Figure* 3 *for a degree of these mapes.*

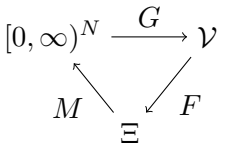

Figure 3. *A diagram of maps from* (5).

The set of values Ξ in Definition 2.2 replaces the binary values $0, 1$ that are transmitted in a Boolean network. Note that even when two outward edges from node i have the same sign, say $i \to j$ and $i \to l$, different values can be transmitted to j and l since the values $F_{j,i}(k)$ and $F_{l,i}(k)$ may be different. This generalizes the behavior of a traditional Boolean function.

One serious objection to representing the dynamics of a network by either a Boolean function B or a discrete function D is that it does not respect the continuity of the underlying biological process. In particular, the Boolean vector $(B(s) - s)$ can be nonzero in more than one component which implies that two or more processes switch at exactly the same time. In addition, the vector $(D(s) - s)$ can have entries greater than 1 in absolute value, implying that chemical concentrations change from one state to a nonadjacent state, without attaining intermediate values corresponding to intermediate states. This violates continuity of the underlying chemical process. An *asynchronous update* of Boolean functions B has been proposed [12, 37] to generate dynamics that are compatible with continuous variables, and we extend this approach to the map D.

For a given multilevel discrete map D we define a nearest neighbor multivalued map $\mathcal{F}$, that only allows transitions from domains to the adjacent domains in phase space, where these transitions are induced by D.

Definition 2.3. *Let s_1 and s_2 be the states of two domains κ_1 and κ_2, $s_1 = g(\kappa_1)$ and $s_2 = g(\kappa_2)$ from* (2). *These domains are* adjacent along i *(and so are the states) if and only if there exists exactly one index i and exactly one $j \in \mathbf{T}(i)$ such that*

$$\pi_i(\kappa_1) \cap \pi_i(\kappa_2) = \theta_{j,i} \text{ and } \pi_k(\kappa_1) = \pi_k(\kappa_2) \text{ for all } k \neq i.$$

A nearest neighbor multivalued map $\mathcal{F} : \mathcal{V} \rightrightarrows \mathcal{V}$ *is a map such that $u \in \mathcal{F}(s)$ only if*

(a) $s = t = u$, *or*

(b) u *and* s *are adjacent along* i *for some* i.

Definition 2.4. *The* asynchronous update rule of D *is a nearest neighbor multivalued map $\mathcal{F} : \mathcal{V} \rightrightarrows \mathcal{V}$ (see Figure 4) additionally satisfying the property that $u \in \mathcal{F}(s)$ if and only if, whenever $t = D(s)$, we have either*

(a) $s_i < u_i \leq t_i$, *or*

(b) $s_i > u_i \geq t_i$,

where $s := (s_1, s_2, \ldots, s_N)$ and $u := (u_1, u_2, \ldots, u_N)$ are adjacent along i.

$\mathcal{F}$ is sometimes represented as a directed graph, called a state transition graph, *$(\mathcal{V}, \mathcal{E})$, where $(s, u) \in \mathcal{E}$ if and only if $u \in \mathcal{F}(s)$.*

Since the number of states in $\mathcal{V}$ can be very large, it will be useful to capture the dynamics of iterates of $\mathcal{F}$ by a more compact representation [37, 16], which we proceed to define.

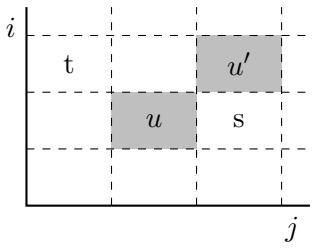

Figure 4. *Illustration of rule* (b) *in Definition 2.4. When the map D takes s to t, then the map $\mathcal{F}$ takes s to a set of states $\{u, u'\}$. States s and u are adjacent along j, and s and u' are adjacent along i.*

Definition 2.5. *A* recurrent component *of the map $\mathcal{F}$ is a* strongly connected path component *of the associated graph $(\mathcal{V}, \mathcal{E})$. In other words, it is a maximal collection of vertices $\mathcal{C} \subset \mathcal{V}$ such that for any $u, v \in \mathcal{C}$ there exists a directed path from u to v with vertices in $\mathcal{C}$ and edges in $\mathcal{E}$. In the context of dynamical systems we refer to a recurrent component of $\mathcal{F}$ as a* Morse set *of $\mathcal{F}$ and denote it by $\mathcal{M} \subset \mathcal{V}$. The collection of all recurrent components of $\mathcal{F}$ is denoted by*

$$\mathsf{MD}(\mathcal{F}) := \{\mathcal{M}(p) \subset \mathcal{V} \mid p \in \mathsf{P}\}$$

and is called a Morse decomposition *of $\mathcal{F}$, where P is an index set. Recurrent components inherit a well-defined partial order from the reachability relation in the directed graph $(\mathcal{V}, \mathcal{E})$. Specifically, we may write the partial order on the indexing set P of $\mathsf{MD}(\mathcal{F})$ by defining*

$$q \preceq p \quad \textit{if there exists a path in } (\mathcal{V}, \mathcal{E}) \textit{ from an element of } \mathcal{M}(p) \textit{ to an element of } \mathcal{M}(q).$$

Definition 2.6. *The* Morse graph *of $\mathcal{F}$, denoted $\mathsf{MG}(\mathcal{F})$, is the Hasse diagram of the poset $(\mathsf{P}, \preceq)$. We refer to the elements of P as the* Morse nodes *of the graph.*

An intriguing question is the characterization of the set of ODEs models that are compatible with a given map $\mathcal{F}$. This class of equations will share the same broad dynamical features that are captured by the Morse graph of $\mathcal{F}$. In the other direction, identifying a map $\mathcal{F}$ for a given ODE system would facilitate its analysis, because of the inherent computability of the Morse graph from the map $\mathcal{F}$.

Definition 2.7. *We say an ODE model with variables x_i and a nearest neighbor multivalued map $\mathcal{F}$ are* compatible *if solutions $x(t)$ can traverse from domain κ_1 to adjacent domain κ_2 only if $s_2 \in \mathcal{F}(s_1)$.*

It is worth noting that we do not require that if $s_2 \in \mathcal{F}(s_1)$, there must be a solution that traverses from κ_1 to κ_2. Investigation of when such solutions exist is a challenging problem that remains open.

2.1. S-systems. Given a regulatory network $\mathbf{RN} = (V, E)$, to each node i we assign a parameter γ_i^S, which will be interpreted as a rate of degradation of x_i. For each edge $(i, j) \in E$ we associate three numbers: a threshold $\theta_{j,i}$ a low value $l_{j,i}^S$ and a high value $u_{j,i}^S$, so that $\Xi_{j,i} = \{l_{j,i}^S, u_{j,i}^S\}$ (see Definition 2.2). We require for all i that

$$0 < \gamma_i^S, \quad 0 < l_{j,i}^S < u_{j,i}^S, \quad 0 < \theta_{j,i}, \quad \theta_{j,i} \neq \theta_{k,i} \text{ whenever } j \neq k$$

and we call an *S-parameter* of **RN** the tuple $z^S = (l^S, u^S, \theta, \gamma^S) \in \mathbb{R}^{d^S}$, where $d^S = \#(V) + 3\#(E)$.

At every S-parameter and for every $i = 1, \dots, N$, the interval $[0, \infty)$ can be decomposed into intervals with nonoverlapping interiors

$$(I_{0,i} := [0, \theta_{j_1,i}]) \le (I_{1,i} := [\theta_{j_1,i}, \theta_{j_2,i}]) \le \cdots \le (I_{m_i,i} := [\theta_{j_{m_i},i}, \infty)), \quad m_i = |\mathbf{T}(i)|,$$

since the thresholds form a linearly ordered set $\{\theta_{\ell,i} : \ell \in \mathbf{T}(i)\} \subset [0, \infty)$. While intervals $I_{k,i}$ are ordered according to the first subscript, the first subscript of the threshold $\theta_{j_k,i}$ refers to the identity of the target node j_k associated with the edge $i \to j_k$ in **RN**.

We define the ith component of the state function G^S (see (1)) by

$$G_i^S(x_i) = k \text{ when } x_i \in \operatorname{int} I_{k,i}.$$

We leave $G_i^S(x_i)$ undefined on the finite set of values $x_i = \theta_{n,i}$, $n = j_1, \dots, j_{m_i}$. We denote the range of G^S by $\mathcal{V}^S$, which is the product of sets $\{0, \dots, m_i\}$ (see Definition 2.2).

Let $I_{k,i} = [\theta_{j_k,i}, \theta_{j_{k+1},i}]$ be the kth interval with $j := j_k$ so that $G_i^S(x_i) < k$ implies $x_i < \theta_{j,i}$. We define $F_{j,i}^S$ from (3) as

$$F_{j,i}^S \circ G_i^S(x_i) := \begin{cases} l_{j,i}^S & \text{if } G_i^S(x_i) < k \text{ and } i \to j, \text{ or } G_i^S(x_i) \ge k \text{ and } i \dashv j, \\ u_{j,i}^S & \text{for } G_i^S(x_i) \ge k \text{ and } i \to j, \text{ or } G_i^S(x_i) < k \text{ and } i \dashv j, \\ \text{undefined} & \text{if } x_i = \theta_{n,i} \text{ for } n = j_1, \dots, j_{m_i}. \end{cases} \tag{6}$$

Let $\sigma_{j,i}^S := F_{j,i}^S \circ G_i^S(x_i)$ and let σ_j^S be the vector-valued function with components $\sigma_{j,i}^S$. We will refer to components of σ_j^S as *regulatory functions*.

Finally, to every node j we assign a rule $\bar{M}_j$ that combines the values of σ_j^S into real numbers. This rule is called a *logic function* at the node j, following the nomenclature and construction of [16], and it is assumed to be a multiaffine function with all coefficients equal to 1. Recall that a multiaffine function is a polynomial with the property that the degree in any of its variables is at most 1. We set

$$\Lambda_j^S(x) := \bar{M}_j \circ \sigma_j^S(x).$$

The *S-system for **RN*** is a collection of ODEs of the following form

$$\dot{x}_j = -\gamma_j^S x_j + \Lambda_j^S(x) = -\gamma_j^S x_j + \bar{M}_j \circ \sigma_j^S(x), \qquad j = 1, \dots, N, \tag{7}$$

with a fixed network **RN** and a fixed logic function $\bar{M}_j$. However, the values of parameters $z^S = (l^S, u^S, \theta, \gamma^S) \in \mathbb{R}^{d^S}$ are not specified. By substituting a particular S-parameter, $z^S \in \mathbb{R}^{d^S}$, a particular ODE system is given, which we refer to as a *parameterized S-system (for **RN**)*. The collection of all S-systems for all possible networks and logic functions is the *class of S-systems*.

Define $D^S : \mathcal{V}^S \to \mathcal{V}^S$ by

$$D^S := G^S \circ \Gamma^{-1} \Lambda^S \circ (G^S)^{-1},$$

where Γ is the diagonal matrix containing γ_i^S, and Λ^S, $\bar{M}$, and σ^S are the vector-valued functions with components Λ_j^S, $\bar{M}_j$, and σ_j^S, respectively. From the definition of σ^S we have

$$G^S \circ \Gamma^{-1}\Lambda^S = G^S \circ \Gamma^{-1}\bar{M} \circ \sigma^S = G^S \circ M \circ F^S \circ G^S,$$

where we define the combination function $M := \Gamma^{-1}\bar{M}$ (see Definition 2.2) to be a scaled version of the logic function $\bar{M}$. Then,

$$D^S = G^S \circ M \circ F^S, \tag{8}$$

which matches (5). We show later that this multilevel discrete map D^S has a procedure for generating an associated asynchronous update rule $\mathcal{F}^S$ that is compatible with a given parameterized S-system.

Throughout this paper, whenever we refer to the S-system, a fixed **RN** is always assumed to be implied by the context.

Continuing the example **RN** shown in Figure 2, the corresponding S-system is

$$\dot{x} = -\gamma_x^S x + \sigma_{x,y}^S(y),$$
$$\dot{y} = -\gamma_y^S y + \sigma_{y,x}^S(x),$$

where

$$\sigma_{x,y}^S(y) = \begin{cases} u_{x,y}^S, & \text{if } y < \theta_{x,y}, \\ l_{x,y}^S, & \text{if } y > \theta_{x,y}^S, \end{cases} \qquad \sigma_{y,x}^S(x) = \begin{cases} u_{y,x}^S & \text{if } x < \theta_{y,x}, \\ l_{y,x}^S & \text{if } x > \theta_{y,x}. \end{cases}$$

The function $\sigma_{y,x}^S(x)$ is depicted on the left in Figure 1. The other function $\sigma_{x,y}^S(y)$ will have the same shape, as both edges of the example **RN** correspond to negative regulation. Making a substitution of particular values (e.g., $l_{y,x}^S = 1.8, u_{y,x}^S = 5.3, \gamma_y^S = 17$, etc.) would result in a parameterized S-system.

2.2. L-systems. For the L-system we replace a single threshold $\theta_{j,i}$ by two thresholds $\vartheta_{j,i}^-$ and $\vartheta_{j,i}^+$. Given a regulatory network $\mathbf{RN} = (V, E)$, to each node i we again assign a decay parameter γ_i^L. For each edge $(i, j) \in E$, we associate four real-valued parameters $u_{j,i}^L$, $l_{j,i}^L$, $\vartheta_{j,i}^-$, and $\vartheta_{j,i}^+$, where again $\Xi_{j,i} := \{l_{j,i}^L, u_{j,i}^L\}$ (Definition 2.2). We require for all i that

$$0 < \gamma_i^L, \quad 0 < l_{j,i}^L < u_{j,i}^L, \quad 0 < \vartheta_{j,i}^- < \vartheta_{j,i}^+, \quad [\vartheta_{j,i}^-, \vartheta_{j,i}^+] \cap [\vartheta_{k,i}^-, \vartheta_{k,i}^+] = \emptyset \text{ whenever } j \neq k.$$

The tuple $z^L = (l^L, u^L, \vartheta^-, \vartheta^+, \gamma^L) \in \mathbb{R}^{d^L}$ is an *L-parameter of* **RN**, where $d^L = \#(V) + 4\#(E)$.

In an analogy with the S-system, we define a regulatory function $\sigma_j^L(x)$, which is a vector-valued function with coordinates $\sigma_{j,i}^L(x)$, given by

$$\sigma_{j,i}^L(x) := \begin{cases} l_{j,i}^L & \text{for } x_i \le \vartheta_{j,i}^- \text{ and } i \to j, \text{or } x_i \ge \vartheta_{j,i}^+ \text{ and } i \dashv j, \\ u_{j,i}^L & \text{for } x_i \ge \vartheta_{j,i}^+ \text{ and } i \to j, \text{or } x_i \le \vartheta_{j,i}^- \text{ and } i \dashv j, \\ f_{j,i}^L(x_i) & \text{for } x_i \in [\vartheta_{j,i}^-, \vartheta_{j,i}^+], \end{cases} \tag{9}$$

where $f^L_{j,i}(x_i)$ is a Lipschitz continuous function with lower bound $l^L_{j,i}$ and upper bound $u^L_{j,i}$, and makes $\sigma^L_{j,i}(x)$ continuous. The function $\sigma^L_{j,i}(x)$ is a step function that is regularized by a Lipschitz bridge. This defines a vector-valued function $\sigma^L_j(x)$ coordinatewise.

Definition 2.8. *At every L-parameter and for every $i = 1, \dots, N$, the interval $[0, \infty)$ is decomposed into intervals with nonoverlapping interiors*

$$(I_{0,i} := [0, \vartheta^-_{j_1,i}]) \le (I_{\frac{1}{2},i} := [\vartheta^-_{j_1,i}, \vartheta^+_{j_1,i}]) \le (I_{1,i} := [\vartheta^+_{j_1,i}, \vartheta^-_{j_2,i}]) \le \cdots \le (I_{m_i,i} := [\vartheta^-_{j_{m_i},i}, \infty)).$$

We define the ith component of the state function G^L (see (1)) by

$$G^L_i(x_i) = k \text{ when } x_i \in \operatorname{int} I_{k,i},$$

where $k \in \{0, \frac{1}{2}, 1, \frac{3}{2}, 2, \dots, m_i\}$. We leave $G^L_i(x_i)$ undefined on a finite set of values $x_i = \vartheta^{\pm}_{n,i}$, where $n = j_1, \dots, j_{m_i}$.

Notice that, unlike G^S, the range of G^L includes also half-integers. This will facilitate a definition of a mapping between the systems that will be introduced in section 4.

The *L-system for* $\boldsymbol{RN}$ is a collection of ODEs of the following form,

$$\dot{x}_j = -\gamma^L_j x_j + \Lambda^L_j(x) = -\gamma^L_j x_j + \bar{M}_j \circ \sigma^L_j(x), \qquad j = 1, \dots, N, \tag{10}$$

where $\bar{M}_j$ is defined as for an S-system. Like the S-system, an L-system is a collection of ODE systems with a fixed network **RN** and a fixed logic function $\bar{M}_j$. By substituting a particular L-parameter into the L-system we obtain a *parameterized L-system*. However there is a key difference between the L- and S-systems. A parameterized L-system is in fact a class of ODE systems, as the exact form of $f^L_{j,i}(x_i)$ has not been specified. We do this because the results of this paper apply to all functions $f^L_{j,i}(x_i)$ for a given parameterized L-system with a fixed L-parameter. We emphasize that $f^L_{j,i}(x_i)$ does not have to take any particular form (for example, piecewise linear, piecewise sigmoid, etc.), and in fact can be very nonlinear, as long as it satisfies the given conditions. We call the collection of all L-systems the *class of L-systems*.

It is important to note that the function $\sigma^L_{j,i}(x)$ cannot be represented as a composition $F^L_{j,i} \circ G^L_i$ as in the S-system. This is because the range of $\sigma^L_{j,i}$ is an interval $[l^L_{j,i}, u^L_{j,i}]$, rather than the discrete set of values $\{l^L_{j,i}, u^L_{j,i}\}$. This means that we cannot construct a multilevel discrete function D^L. However, we will construct a nearest neighbor multivalued map $\mathcal{F}^L$ such that the solutions of a parameterized L-system are compatible with $\mathcal{F}^L$. In section 4, we will, however, construct a multilevel discrete map D^L_N with a restricted domain in order to compare the nearest neighbor multivalued maps $\mathcal{F}^S$ and $\mathcal{F}^L$.

We continue our example. For the network shown in Figure 2, the associated L-system is given by

$$\dot{x} = -\gamma^S_x x + \sigma^L_{x,y}(y),$$
$$\dot{y} = -\gamma^S_y y + \sigma^L_{y,x}(x).$$

In Figure 1 (right) we depict one possible shape of the function $\sigma^L_{i,j}(x_j)$; any Lipschitz-continuous function $f^L_{i,j}(x_j)$ that connects $u^L_{y,x}$ and $l^L_{y,x}$ and is bounded vertically between these also satisfies our constraints on $\sigma^L_{i,j}(x_j)$.

3. Construction of $\mathcal{F}^S$ and $\mathcal{F}^L$. In this section we will show that both the S- and L-systems generate nearest neighbor multivalued maps $\mathcal{F}^S$ and $\mathcal{F}^L$ (see Definition 2.3). We will represent these maps as graphs with vertices that correspond to discrete states, and edges that correspond to allowed transitions.

It is clear from the definition of the S-system that the thresholds $\{\theta_{j,i} : j \in \mathbf{T}(i)\}$ form a strict total order for each $i \in V$. We denote this collection of orderings by $O(z^S)$. Similarly, the intervals $\{[\vartheta^-_{j,i}, \vartheta^+_{j,i}] : j \in \mathbf{T}(i)\}$ form a strict total order for each $i \in V$, and we denote the collection by $O(z^L)$. Note that Λ^S_j and Λ^L_j from (7) and (10) are multiaffine combinations of bounded functions, so they are themselves bounded. For convenience we introduce the thresholds $\vartheta_{0,i} = \theta_{0,i} = 0$ and $\vartheta_{\infty,i} = \theta_{\infty,i} = \infty$ for each i.

Definition 3.1. *Let φ_i, φ'_i be two thresholds in either the parameterized S- or L-systems for some x_i. We say that φ_i, φ'_i are* adjacent *if $\varphi_i < \varphi'_i$ and there does not exist φ''_i such that $\varphi_i < \varphi''_i < \varphi'_i$.*

Let

$$\zeta := \prod_{i=1}^{N} I_i,$$

where I_i is either a nondegenerate interval $I_i = [\varphi_i, \varphi'_i]$ with adjacent thresholds φ_i, φ'_i, a half-infinite interval $I_i = [\varphi_i, \infty)$, where φ_i is the largest of the thresholds of x_i, or a degenerate interval $I_i = [\varphi_i, \varphi_i]$. Let

$$ND(\zeta) := \{i \in \{1, \dots, N\} \mid I_i \text{ is a nondegenerate interval}\},$$

and let $\ell = \#(ND(\zeta))$. Since ζ has dimension ℓ in phase space we will call ζ an ℓ-cell.

We reserve a special symbol κ for an N-cell which we will refer to as a domain. The collection of all domains of the parameterized S-system will be denoted by $\mathcal{K}^S$ and the same collection for the parameterized L-system will be $\mathcal{K}^L$.

In order to facilitate comparison between domains of parameterized S- and L-systems we define two subsets of $\mathcal{K}^L$. First, we denote $\mathcal{K}^L_N \subsetneq \mathcal{K}^L$ to be the set of domains κ such that for every $i \in ND(\kappa)$, the interval I_i is either half-infinite or of the form $I_i = [\vartheta^+_{j_m,i}, \vartheta^-_{j_{m+1},i}]$. These are the intervals where the regulatory functions $\sigma^L_{j,i}(x_i)$ are constant. Second, we define the subset $\mathcal{K}^L_{N-1} \subsetneq \mathcal{K}^L$ such that one and exactly one $\sigma^L_{j,i}(x_i)$ is not constant; that is, there is exactly one $i \in ND(\kappa)$ such that $I_i = [\vartheta^-_{j,i}, \vartheta^+_{j,i}]$ for some j.

See Figure 5 for examples of domains in the S- and L-systems.

We now define terms related to the boundary of an N-cell.

Definition 3.2. *Let $\kappa \in \mathcal{K}^S$ or $\kappa \in \mathcal{K}^L$. We say that*

$$\tau^-_j := \prod_{i=1}^{j-1} I_i \times [\varphi_j, \varphi_j] \times \prod_{i=j+1}^{N} I_i$$

is a left face *of κ with* projection index *j. In other words, $\tau^-_j \subset \{x \mid x_j = \varphi_j\}$. Similarly, if $\varphi'_j \neq \infty$, we say that*

$$\tau^+_j := \prod_{i=1}^{j-1} I_i \times [\varphi'_j, \varphi'_j] \times \prod_{i=j+1}^{N} I_i$$

is a right face *of κ with projection index j. In other words, $\tau^+_j \subset \{x \mid x_j = \varphi'_j\}$.*

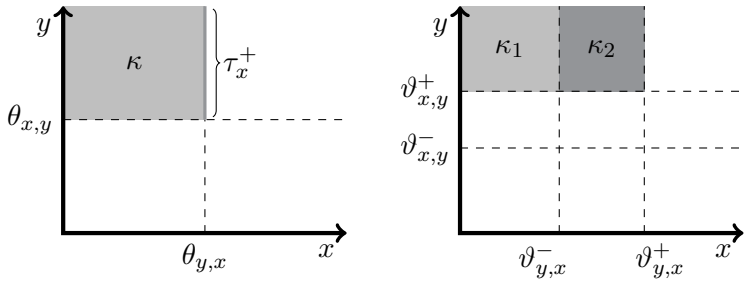

Figure 5. *Phase space for the S-system (left), and L-system (right) associated with* ***RN*** *in Figure 2. For the S-system, a domain κ is shown in light gray, with its right face, τ_x^+, shown in dark gray. For the L-system, two domains are shown, κ_1 in light gray, and κ_2, in dark gray. Here $\kappa_1 \in \mathcal{K}_N^L$ and $\kappa_2 \in \mathcal{K}_{N-1}^L$ for $N = 2$.*

A wall is a pair (τ, κ), where κ is a domain and τ is a face of κ. Each wall inherits the projection index from the corresponding face τ of κ. We say the sign of the wall (τ, κ) is 1 (and write $sgn(\tau, \kappa) = 1$) if τ is a left face of κ and we say the sign of the wall (τ, κ) is -1 (and write $sgn(\tau, \kappa) = -1$) if τ is a right face of κ. Note that since both κ and τ carry identity of the thresholds that bound them, the collection of walls depends on the parameter z. We therefore denote the collection of walls at parameter z by $\mathcal{W}(z)$.

See Figure 5 (left) for an example of a right face.

The goal of this section is to define maps $\mathcal{F}^S$ and $\mathcal{F}^L$ on a discrete set of states. The states will be associated with domains $\mathcal{K}^S$ and $\mathcal{K}^L$. For each pair of domains κ, κ' such that $\tau = \kappa \cap \kappa'$ is a face with some projection index j, we will associate a direction, either $+1, -1$, or both, with each pair of walls (τ, κ) and (τ, κ') by making use of the sign of these walls. We then finish by associating an oriented edge (or edges) with the pair of states that correspond to κ and κ'.

Observe that by definition of functions $\Lambda(x)$ for either parameterized S- or L-systems, ((7) and (10)), the value of $\Lambda(x)$ is constant on the interior $\text{int}(\kappa)$ of κ, where $\kappa \in \mathcal{K}^S$ for the parameterized S-system or $\kappa \in \mathcal{K}_N^L$ for the parameterized L-system. We emphasize that this is not true for domains $\kappa \in \mathcal{K}^L \setminus \mathcal{K}_N^L$ for parameterized L-systems, since there is at least one variable $x_i \in [\vartheta_{j,i}^-, \vartheta_{j,i}^+]$ that lies in the interval where function $\sigma_{j,i}^L$ is nonconstant.

With a slight abuse of the notation we will call this value $\Lambda(\kappa)$. The value

$$\Lambda(\kappa) = (\Lambda_1(\kappa), \ldots, \Lambda_N(\kappa))$$

has a nice interpretation in terms of solutions of the parameterized S-system: all solutions starting at $x \in \text{int}(\kappa)$ converge toward the point

$$\Gamma^{-1}\Lambda^S(\kappa) = (\Lambda_1^S(\kappa)/\gamma_1^S, \ldots, \Lambda_N^S(\kappa)/\gamma_N^S),$$

where Γ is a diagonal matrix consisting of γ_i^S. Whenever context is clear, we will write Γ^{-1} instead of $(\Gamma^S)^{-1}$ or $(\Gamma^L)^{-1}$ to avoid double superscripts.

Definition 3.3. *The* focal point *or* target *point of a domain $\kappa \in \mathcal{K}^S$ at an S-parameter or $\kappa \in \mathcal{K}_N^L$ at an L-parameter is the value $\Gamma^{-1}\Lambda(\kappa)$. If $\Gamma^{-1}\Lambda(\kappa) \in \kappa'$ we call κ' a* target domain. *We say that κ is an* attracting domain *if $\Gamma^{-1}\Lambda(\kappa) \in \kappa$.*

Definition 3.4. *A* regular S-parameter z^S *satisfies for all* $i = 1, \dots, N$, $j \in \mathbf{T}(i)$, *and* $\kappa \in \mathcal{K}^S$,

$$\Lambda_i^S(\kappa)/\gamma_i^S \neq \theta_{j,i}.$$

We call the space of all regular S-parameters Z^S.

A regular L-parameter z^L *satisfies for all* $i = 1, \dots, N$, $j \in \mathbf{T}(i)$, *and* $\kappa \in \mathcal{K}_N^L$,

$$\Lambda_i^L(\kappa)/\gamma_i^L \neq \vartheta_{j,i}^{\pm}.$$

We call the space of all regular L-parameters Z^L.

3.1. Nearest neighbor multivalued map $\mathcal{F}^S$ for the S-system. We now proceed to construct a nearest neighbor multivalued map $\mathcal{F}^S$ from the focal points of the parameterized S-system (7), then we show that $\mathcal{F}^S$ is compatible with the parameterized S-system in the sense of Definition 2.7, and, finally, we show that $\mathcal{F}^S$ is an asynchronous update rule for D^S defined in (8).

Definition 3.5 (see [16]). *Let* z^S *be a regular S-parameter and* $\mathcal{K}^S$ *the corresponding set of domains. The* wall labeling *of* $\mathcal{W}(z^S)$ *is a function* $\mathscr{L}^S : \mathcal{W}(z^S) \to \{-1, 1\}$ *defined as follows. Let* $(\tau, \kappa) \in \mathcal{W}(z^S)$ *be a wall with projection index* i; *i.e.,* $\tau \subset \{x \mid x_i = \theta_{j,i}\}$. *Then define*

$$\mathscr{L}^S((\tau, \kappa)) := sgn(\tau, \kappa) \cdot sgn(\Lambda_i^S(\kappa)/\gamma_i^S - \theta_{j,i}).$$

A wall (τ, κ) *is an* absorbing (exit) wall *if* $\mathscr{L}^S((\tau, \kappa)) = -1$ *and an* entrance wall *if* $\mathscr{L}^S((\tau, \kappa)) = 1$.

Notice that a regular parameter enforces $\Lambda_i^S(\kappa)/\gamma_i - \theta_{j,i} \neq 0$, so that every wall is either an absorbing wall or an entrance wall.

For the next definition, recall from section 2.1 that $\mathcal{V}^S := \prod_{i=1}^N \{0, 1, \dots, m_i\}$ is the range of the state function $G^S(x)$ with components $G_i^S(x_i)$.

Definition 3.6. *Let* z^S *be a regular S-parameter and let* $\mathcal{K}^S$ *be the corresponding set of domains. Let*

$$g^S : \mathcal{K}^S \to \mathcal{V}^S$$

be a bijection defined by $g^S(\kappa) = (G_1^S(x_1), \dots, G_N^S(x_N))$ *for any* $(x_1, \dots, x_N) \in \kappa$ *(see (2)).*

We define a multivalued map $\mathcal{F}^S : \mathcal{V}^S \rightrightarrows \mathcal{V}^S$ *induced by the wall labeling* $\mathscr{L}^S$ *as follows. Let* $g^S(\kappa_1) = s_1$ *and* $g^S(\kappa_2) = s_2$. *Then* $s_2 \in \mathcal{F}^S(s_1)$ *if and only if one of the following holds:*

(a) $s_1 = s_2$ *and* κ *is an attracting domain.*

(b) *There exists some face* τ *such that* (τ, κ_1) *and* (τ, κ_2) *are walls and* $\mathscr{L}^S((\tau, \kappa_1)) = -1$ *(indicating an absorbing wall of* κ_1*) and* $\mathscr{L}^S((\tau, \kappa_2)) = 1$ *(indicating an entrance wall of* κ_2*).*

As in Definition 2.4 we may represent $\mathcal{F}$ *as a graph* $(\mathcal{V}^S, \mathcal{E}^S)$, *where* $(s_1, s_2) \in \mathcal{E}^S$ *if and only if* $s_2 \in \mathcal{F}^S(s_1)$. *We call this graph the state transition graph of the parameterized S-system. The state transition graph is unique for a given parameterized S-system.*

Theorem 3.7. $\mathcal{F}^S$ *is compatible with the corresponding parameterized S-system.*

Proof. The key observation is that all solutions in $\text{int}(\kappa)$ converge toward the target point $\Gamma^{-1}\Lambda^S(\kappa)$, while they lie within κ. If there is no trajectory leaving κ for an adjacent domain, then the trajectory x must remain within κ for all time. Hence the focal point $\Gamma^{-1}\Lambda^S(\kappa)$ is in κ, and κ is an attracting domain. By Definition 3.6(a), $s \in \mathcal{F}^S(s)$, where $s = g^S(\kappa)$.

Now assume that there exists a trajectory $x(t) = (x_1(t), \dots, x_N(t))$ that passes from κ_1 to an adjacent κ_2 via an intervening face τ, where $x_i = \theta_{j,i}$ on τ. First consider the case in which τ is a right face of κ_1 and a left face of κ_2, so that $\text{sgn}(\tau, \kappa_1) = -1$ and $\text{sgn}(\tau, \kappa_2) = 1$. Let $x_i(0) = \theta_{j,i}$. There is an interval $I := (-\epsilon, \epsilon) \subset \mathbb{R}$ such that $\dot{x}_i(t) > 0$ for all $t \in I \setminus \{0\}$ and $x(t) \in \kappa_1$ for $t \in (-\epsilon, 0)$, $x(t) \in \kappa_2$ for $t \in (0, \epsilon)$. Let $T_k = \Lambda_i^S(\kappa_k)/\gamma_i^S$ for $k = 1, 2$ denote the ith component of the target points of the domains. Then $\dot{x}_i(t) > 0$ for all $t \in I \setminus \{0\}$ implies $T_1, T_2 > \theta_{j,i}$, which implies

$$\mathscr{L}^S((\tau, \kappa_1)) = -1 \cdot 1 \text{ and } \mathscr{L}^S((\tau, \kappa_2)) = 1 \cdot 1.$$

Thus $s_2 \in \mathcal{F}^S(s_1)$, where $s_k := g^S(\kappa_k)$, by Definition 3.6(b). The case in which $\text{sgn}(\tau, \kappa_1) = 1$ and $\text{sgn}(\tau, \kappa_2) = -1$ with $\dot{x}_i(t) < 0$ for $t \in I \setminus \{0\}$ is similar. ∎

Recall that the multilevel discrete map for a parameterized S-system, D^S was defined in (8). The proof of the following theorem we postpone to Appendix A.

Theorem 3.8. *$\mathcal{F}^S$ is an asynchronous update rule for D^S.*

3.2. Nearest neighbor multivalued map $\mathcal{F}^L$ for the L-system. While Definition 3.3 defines focal points for all domains $\kappa \in \mathcal{K}^S$, it only does so for domains $\kappa \in \mathcal{K}_N^L \subsetneq \mathcal{K}^L$ in the parameterized L-system. Therefore, we cannot construct a multilevel discrete map D^L analogous to D^S for the parameterized S-system. Moreover, the wall labeling that we used to construct $\mathcal{F}^S$ cannot be used in the same way for $\kappa \in \mathcal{K}^L$ to define $\mathcal{F}^L$. But it turns out that all the information needed to assign directions to all walls in the L-system can be inferred from just the domains in $\mathcal{K}_N^L$. We will use this fact to construct a nearest neighbor multivalued map $\mathcal{F}^L$ and associated state transition graph $(\mathcal{V}^L, \mathcal{E}^L)$, without going through a multilevel discrete map D^L as an intermediary.

For the next definition, recall from Definition 3.1 that an ℓ-cell has the form $\zeta = \prod_{i=1}^N [\varphi_i, \varphi_i']$, where for exactly ℓ indices we have $\varphi_i \neq \varphi_i'$.

Definition 3.9. *We define the set of* corner points *of ζ, denoted $\mathcal{C}(\zeta)$, by*

$$\mathcal{C}(\zeta) := \prod_{i=1, \varphi_i' \neq \infty}^{N} \{\varphi_i, \varphi_i'\}.$$

Note that we exclude $\varphi_i' = \infty$ from the definition of corner points.

Definition 3.10. *Let $\mathcal{C}(\zeta)$ be the set of corner points for an ℓ-cell ζ for a parameterized L-system with regular L-parameter z^L. We introduce the function $\texttt{Sign}(\mathcal{C}(\zeta), k)$ defined as* (11)

$$\texttt{Sign}(\mathcal{C}(\zeta), k) = \begin{cases} +1 & \text{if } \forall P \in \mathcal{C}(\zeta), \Lambda_k^L(P)/\gamma_k - \varphi_k > 0 \\ -1 & \text{if } \forall P \in \mathcal{C}(\zeta), \Lambda_k^L(P)/\gamma_k - \varphi_k < 0 \\ 0 & \text{if } \exists P, P' \in \mathcal{C}(\zeta) \text{ such that } \Lambda_k^L(P)/\gamma_k - \varphi_k > 0 \text{ and } \Lambda_k^L(P')/\gamma_k - \varphi_k' < 0. \end{cases}$$

Notice that a regular L-parameter enforces $\Lambda_k^L(P)/\gamma_k - \varphi_k \neq 0$, so that (11) covers all possible cases. Note also that since the intervals $[\vartheta_{k,i}^-, \vartheta_{k,i}^+]$ are disjoint for all k, the ith component of every corner point of ζ is on the boundary of the set $\mathbb{R} \setminus \bigcup_k [\vartheta_{k,i}^-, \vartheta_{k,i}^+]$. Therefore every corner point of ζ is also the corner point of some $\kappa \in \mathcal{K}_N^L$.

Definition 3.11. *Let $z^L \in Z^L$ be a regular L-parameter. The* wall labeling *of $\mathcal{W}(z^L)$ is a function $\mathscr{L}^L : \mathcal{W}(z^L) \to \{-1, 0, 1\}$ defined as follows. Let $(\tau, \kappa) \in \mathcal{W}(z^L)$ have a projection index i. Then define*

$$\mathscr{L}^L((\tau, \kappa)) := sgn(\tau, \kappa) \cdot \texttt{Sign}(\mathcal{C}(\tau), i).$$

A wall (τ, κ) is an absorbing wall *if $\mathscr{L}^L((\tau, \kappa)) = -1$, an* entrance wall *if $\mathscr{L}^L((\tau, \kappa)) = 1$, and a* bidirectional wall *if $\mathscr{L}^L((\tau, \kappa)) = 0$.*

Recall from Definition 2.8 that $\mathcal{V}^L := \prod_{i=1}^N \{0, \frac{1}{2}, 1, \frac{3}{2}, 2, \dots, m_i\}$ is the range of the state function $G^L(x)$ with components $G_i^L(x_i)$.

Definition 3.12. *Let z^L be a regular L-parameter for a parameterized L-system and let $\mathcal{K}^L$ be the corresponding set of domains. Let*

$$g^L : \mathcal{K}^L \to \mathcal{V}^L$$

be a bijection defined by $g^L(\kappa) = (G_1^L(x_1), \dots, G_N^L(x_N))$ for any $(x_1, \dots, x_N) \in \kappa$ (see (2)).

The nearest neighbor multivalued map $\mathcal{F}^L : \mathcal{V}^L \rightrightarrows \mathcal{V}^L$ induced by the wall labeling $\mathscr{L}^L$ is defined as follows. Let $g^L(\kappa_1) = s_1$ and $g^L(\kappa_2) = s_2$. Then $s_2 \in \mathcal{F}^L(s_1)$ if and only if one of the following holds:

(a) *$s_1 = s_2$ and $\kappa \in \mathcal{K}_N^L$ is an attracting domain.*

(b) *There exists some face τ such that (τ, κ_1) and (τ, κ_2) are walls and $\mathscr{L}^L((\tau, \kappa_1)) = -1$ (indicating an absorbing wall of κ_1) and $\mathscr{L}^L((\tau, \kappa_2)) = 1$ (indicating an entrance wall of κ_2).*

(c) *There exists some face τ such that (τ, κ_1) and (τ, κ_2) are walls and $\mathscr{L}^L((\tau, \kappa_1)) = \mathscr{L}^L((\tau, \kappa_2)) = 0$ (indicating a bidirectional wall of both κ_1 and κ_2).*

We make two notes about this definition.

- First, since attracting domains are only defined for $\kappa \in \mathcal{K}_N^L \subsetneq \mathcal{K}^L$ we can have self-edges only on domains. We justify this choice later by showing that there is always an escape path out of any $\kappa \in \mathcal{K}^L \setminus \mathcal{K}_N^L$; see Lemma C.4 and Corollary C.5.
- Second, notice that if there exist two domains κ_1, κ_2 in a parameterized L-system phase space sharing a face τ, then $\mathscr{L}^L((\tau, \kappa_1)) = 0$ if and only if $\texttt{Sign}(\mathcal{C}(\tau), i) = 0$, which happens if and only if $\mathscr{L}^L((\tau, \kappa_2)) = 0$. Therefore there is never a case where $\mathscr{L}^L((\tau, \kappa_1)) \in \{+1, -1\}$ and $\mathscr{L}^L((\tau, \kappa_2)) = 0$. This shows that the multivalued map is well defined.

Theorem 3.13. *$\mathcal{F}^L$ is compatible with the corresponding parameterized L-system.*

Proof. If there is no trajectory leaving $\kappa \in \mathcal{K}_N^L$ for an adjacent domain, then the trajectory x must remain within κ for all time. Hence the focal point $\Gamma^{-1}\Lambda^L(\kappa)$ is in κ, and κ is an attracting domain. By Definition 3.12(a), $s \in \mathcal{F}^S(s)$, where $s = g^S(\kappa)$.

Now assume that there exists a trajectory that passes from κ_1 to an adjacent κ_2 via an intervening face τ. First consider the case in which τ is a right face of κ_1 and a left face of

κ_2, so that $\operatorname{sgn}(\tau, \kappa_1) = -1$ and $\operatorname{sgn}(\tau, \kappa_2) = 1$. Then $\dot{x}_i > 0$ on τ and thus

$$\texttt{Sign}(\mathcal{C}(\tau), i) \in \{0, +1\}$$

since $\texttt{Sign}(\mathcal{C}(\tau), i) = -1$ implies $\dot{x}_i < 0$ everywhere on τ by Theorem B.2 in the appendix. If $\texttt{Sign}(\mathcal{C}(\tau), i) = +1$, then

$$\mathscr{L}^L((\tau, \kappa_1)) = -1 \cdot 1, \qquad \mathscr{L}^L((\tau, \kappa_2)) = 1 \cdot 1,$$

and $s_2 \in \mathcal{F}^S(s_1)$, where $s_k := g^S(\kappa_k)$, by Definition 3.12(b). Likewise if $\texttt{Sign}(\mathcal{C}(\tau), i) = 0$, then

$$\mathscr{L}^L((\tau, \kappa_1)) = \mathscr{L}^L((\tau, \kappa_2)) = 0,$$

and $s_2 \in \mathcal{F}^S(s_1)$ by Definition 3.12(c).

The case when $\operatorname{sgn}(\tau, \kappa_1) = 1$ and $\operatorname{sgn}(\tau, \kappa_2) = -1$ is similar. ∎

4. Relating $\mathcal{F}^S$ and $\mathcal{F}^L$. We now compare the dynamics of the nearest neighbor multivalued maps $\mathcal{F}^S$ and $\mathcal{F}^L$ that are associated with the same regulatory network $\mathbf{RN} = (V, E)$. Dynamics, in our interpretation, is characterized by the Morse graph (see Definition 2.6) and so our questions will be about the relationship between Morse graphs. $\mathcal{F}^S$ and $\mathcal{F}^L$ are parameterized by $z^S \in Z^S, z^L \in Z^L$ and therefore this comparison must be performed between related parameters. Our goal is to define a canonical map from the set of regular parameters Z^S to the set of regular parameters Z^L.

We make the following key observations:

- For both the parameterized S- and L-systems, the order of the thresholds $\{\theta_{j,i}\}$ for fixed i determines an order of activation (or deactivation) of the targets of node i as x_i increases;
- the images of the maps $\mathcal{F}^S$ and $\mathcal{F}^L$ depend only on the target *domains*, rather than target points in these domains.

Based on these facts, we define an equivalence relation on the set of regular parameters Z^S and an analogous equivalence relation on Z^L.

Definition 4.1 (see [16]). *Let $\boldsymbol{RN}$ be a regulatory network. For each $i \in \{1, \dots, N\}$, let O_i be an ordered set of the targets of node i:*

$$O_i := \{j_1 < j_2 < \cdots < j_{m_i} \mid j_k \in \mathbf{T}(i)\}.$$

Let $O := \{O_i\}_{i=1}^N$ be the collection of these ordered sets.

Let z be a regular parameter of either a parameterized S- or L-system. We say that O is the threshold order *of z, and denote it $O(z)$, if $\theta_{j_k,i} < \theta_{j_l,i}$ in z^S or $[\vartheta^-_{j_k,i}, \vartheta^+_{j_k,i}] < [\vartheta^-_{j_l,i}, \vartheta^+_{j_l,i}]$ in z^L if and only if $j_k < j_l$ in O_i.*

Recall that $\mathcal{V}^S(i) = \{0, 1, 2, \dots, m_i\}$ and $\mathcal{V}^L(i) = \{0, \frac{1}{2}, 1, \frac{3}{2}, 2, \dots, m_i\}$.

Definition 4.2. *We define*

$$\Psi : \mathcal{V}^S \hookrightarrow \mathcal{V}^L \text{ by } \Psi(v) = v, \tag{12}$$

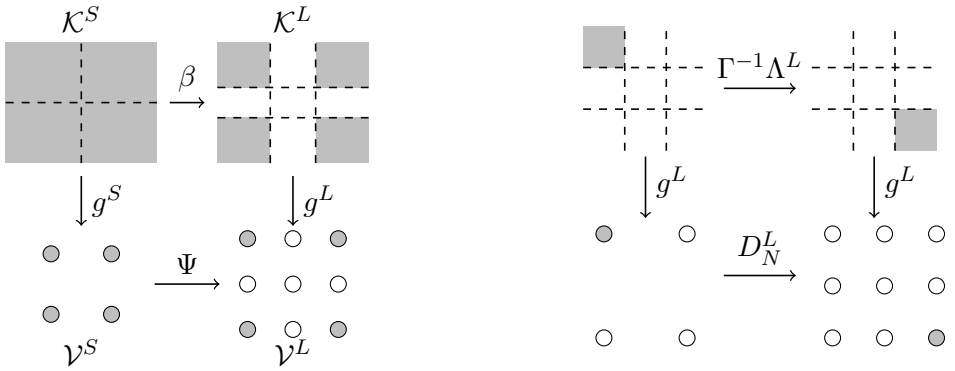

Figure 6. *(Left) A commutative diagram of the maps g^S, g^L, Ψ, and β. The map β is only used in technical lemmas in the appendices, but is included here for completeness. The $\mathcal{K}^S$ and $\mathcal{K}^L$ correspond to the example in Figure 5. The gray shaded region on the top right is the image of β in $\mathcal{K}^L$ and gray dots in the bottom right represent $\mathcal{V}^{SL}$. (Right) Definition of the map $D_N^L := g^L \circ \Gamma^{-1}\Lambda^L(\kappa) \circ (g^L)^{-1}$.*

which is a bijection onto its image $\mathcal{V}^{SL} := \Psi(\mathcal{V}^S)$; see Figure 6(a). We then define a domain-restricted multilevel discrete map D_N^L *(Figure 6(b)) for the L-system by*

$$D_N^L \,:\, \mathcal{V}^{SL} \to \mathcal{V}^L \text{ by } D_N^L := g^L \circ \Gamma^{-1}\Lambda^L(\kappa) \circ (g^L)^{-1}$$

which captures the location of the focal point for each $\kappa \in \mathcal{K}_N^L$.

Since $\mathcal{V}^{SL} = g^L(\mathcal{K}_N^L)$ is a bijection and the target points for $\kappa \in \mathcal{K}_N^L$ are known (see Definition 3.3), the domain-restricted multilevel discrete map D_N^L is well-defined.

Definition 4.3. *We say that two regular parameters $z^S, v^S \in Z^S$ are equivalent,*

$$z^S \overset{S}{\sim} v^S,$$

if the following hold:

(a) $O(z^S) = O(v^S)$ *and*

(b) $D^S(z^S) = D^S(v^S)$, *where $D^S(z^S)$ and $D^S(v^S)$ are the multilevel discrete maps induced by z^S and v^S, respectively (see (8)).*

We denote the equivalence classes of $\overset{S}{\sim}$ by $\mathcal{Z}^S$, and say $\omega^S \in \mathcal{Z}^S$. We shall use the notation $O(\omega^S)$ to denote the constant threshold order for all $z^S \in \omega^S$, and use $D^S(\omega^S)$ to denote the fixed multilevel discrete map valid for all parameters in this equivalence class.

The equivalence relationship $\overset{L}{\sim}$ between $z^L, v^L \in \mathcal{Z}^L$ is defined analogously using the map D_N^L. Notation $\omega^L \in \mathcal{Z}^L$, $O(\omega^L)$, and $D_N^L(\omega^L)$ is also analogous.

Remark 4.4. Note that the maps $\mathcal{F}^S$ and $\mathcal{F}^L$ only depend on the equivalence class ω^S and ω^L, respectively, and not on individual parameters $z^S \in \omega^S$, or $z^L \in \omega^L$. This is because the wall-labeling functions $\mathscr{L}^S$ and $\mathscr{L}^L$ depend only on the location of target points $\Gamma^{-1}\Lambda(\kappa)$ with respect to thresholds. Therefore the Morse graph MG (see Definition 2.5), which we view as a summary of dynamics of $\mathcal{F}$, is also only a function of the equivalence class ω. Since the equivalence classes $\mathcal{Z}^S$ and $\mathcal{Z}^L$ are finite, and the set of permutations of elements of O is finite, it follows that the number of multilevel discrete maps is finite. With a slight abuse of

notation we will denote by $\mathcal{F}^S(\omega^S)$ the map $\mathcal{F}^S$ that corresponds to any parameter $z^S \in \omega^S$. Similar notation will be used for the map $\mathcal{F}^L$.

As an aside, note that the elements of $\mathcal{Z}^S$ correspond to the nodes of a *combinatorial parameter graph*, introduced in [16]. The edges in this graph correspond to a single change in the order of indices in O_i for a single i, or to a change in the ith component from one target state to an adjacent target state for a single i.

Definition 4.5. *The* canonical map $\Omega : \mathcal{Z}^S \hookrightarrow \mathcal{Z}^L$ *maps* $\omega^S \in \mathcal{Z}^S$ *to* $\omega^L \in \mathcal{Z}^L$ *if and only if*
(a) $O(\omega^S) = O(\omega^L)$ *and*
(b) $D^S(\omega^S) = D^L_N(\omega^L)$.

It is easy to see that for a fixed network **RN** the map Ω is injective.

For a fixed network **RN** we have introduced two different classes of multivalued maps $\mathcal{F}^S(\omega^S)$ and $\mathcal{F}^L(\omega^L)$ motivated by parameterized S- and L-systems of differential equations. These are both valid choices of a model that captures the dynamics of the network, and they both describe a family of dynamical models that depend in a continuous way on a high dimensional set of parameters. In Remark 4.4 we commented that the number of dynamical behaviors, as captured by the Morse graphs, is finite, as it only depends on the equivalence class $\omega \in \mathcal{Z}$, and $\mathcal{Z}$ is a finite set. Finally, in Definition 4.5 we constructed a bijection Ω between $\mathcal{Z}^S$ and a subset of $\mathcal{Z}^L$. A natural question is, what is the relationship between the dynamics of $\mathcal{F}^S(\omega)$ and $\mathcal{F}^L(\Omega(\omega))$? More precisely, what is the correspondence between the Morse graphs of $\mathcal{F}^S(\omega)$ and $\mathcal{F}^L(\Omega(\omega))$? The rest of the paper is devoted to this question.

5. Morse graphs of $\mathcal{F}^S(\omega)$ and $\mathcal{F}^L(\Omega(\omega))$.

Before we proceed to the main theorems of the section, we review two sets of technical results that are the basis of the theorems in this section, and proved in the appendix.

- Lemma C.2 and Corollary C.3 state that paths in $(\mathcal{V}^S, \mathcal{E}^S)$ correspond to a select set of paths in $(\mathcal{V}^L, \mathcal{E}^L)$. More precisely, an edge $v \to v'$ in the state transition graph of the S-system exists if and only if the path $\Psi(v) \to u \to \Psi(v')$ exists in the L-system state transition graph, where u corresponds to a unique domain $\eta \in \mathcal{K}^L_{N-1}$. This implies that a path of any length existing in $(\mathcal{V}^S, \mathcal{E}^S)$ can be lifted to a path in $(\mathcal{V}^L, \mathcal{E}^L)$.
- Corollary C.5 of Lemma C.4 proves that every node in $\mathcal{V}^L$ has a path to a node in $\mathcal{V}^{SL} \subset \mathcal{V}^L$. Since self-edges are only added to nodes with no path exiting from them, and all nodes in $\mathcal{V}^L$ that are not in $\mathcal{V}^{SL}$ have at least one path from them, the only nodes that could have self-edges are in $\mathcal{V}^{SL}$. This is our justification for defining self-edges in the L-system state transition graph based only on states corresponding to $\kappa \in \mathcal{K}^L_N = g^{-1}(\mathcal{V}^{SL})$ (see Definition 3.12).

We now proceed to the main theorems of the section that describe the characteristics of a map between the Morse graphs of $\mathcal{F}^S(\omega)$ and $\mathcal{F}^L(\Omega(\omega))$.

Definition 5.1. *A map* $f : X \to Y$ *between ordered spaces* $(X, \leq)$ *and* $(Y, \leq)$ *is* order preserving *if* $x_1 < x_2$ *implies* $f(x_1) \leq f(x_2)$.

Definition 5.2. *Let* $U, V \in \mathsf{MD}$ *be two sets in a Morse decomposition (see Definition 2.5). We define the order* $U \preceq V$ *only if there exists a path from an element* $v \in V$ *to an element* $u \in U$ *in the associated state transition graph of* $\mathcal{F}$. *The inequality is strict if there is no return path.*

Theorem 5.3. *Consider $\omega^S \in \mathcal{Z}^S$ and the nearest neighbor multi-valued maps $\mathcal{F}^S(\omega^S)$ and $\mathcal{F}^L(\Omega(\omega^S))$. Consider the associated Morse decompositions MD^S and MD^L. Then there is the order-preserving map*

$$\phi : \mathsf{MD}^S \to \mathsf{MD}^L, \qquad C' := \phi(C),$$

where C' is the element of MD^L containing the states $\Psi(C) := \{\Psi(v) \mid v \in C\}$; see (12).

Proof. Since $U, V \in \mathsf{MD}^S$, they are strongly connected components of the graph induced by $\mathcal{F}^S$. Strong connectedness implies that for any $u, u' \in U$ there is path from u to u' in U, and likewise there is a path between any $v, v' \in V$. By Corollary C.3 the path between u, u' and the path between v, v' lift to paths in the graph of $\mathcal{F}^L$. Therefore the sets $\Psi(U)$ and $\Psi(V)$ are also strongly connected. Therefore $\Psi(U)$ and $\Psi(V)$ must be subsets of Morse sets in MD^L, say $U', V' \in \mathsf{MD}^L$, respectively. We define $U' := \phi(U)$ and $V' := \phi(V)$.

Finally, if $U \prec V$ in MD^S, there must be a path from an element $v \in V$ to an element $u \in U$. By Corollary C.3 there is a path from $\Psi(v)$ to $\Psi(u)$ in the graph of $\mathcal{F}^L$ and therefore $U' \preceq V'$ in MD^L. This finishes the proof. ∎

Notice that in the proof of Theorem 5.3, we cannot conclude that if $U \prec V$ then $U' \prec V'$, only that $U' \preceq V'$. As we will see later, it may be that $U \prec V$ but $U' = V'$. Theorem 5.3 shows that the general ordering of Morse sets remains similar between the two systems; however, the property of order preservation is not very strong. We will examine ways that we can strengthen this result, as well as reasons why this fails in the general case.

Definition 5.4. *An attractor in a Morse decomposition MD (see Definition 2.5) is a minimal element in the partial order, represented by its Morse set $A \in \mathsf{MD}$. The collection of all attractors of MD^* of the map $\mathcal{F}^*(\omega)$ at $\omega \in \mathcal{Z}^*$ will be denoted by $\mathcal{A}^*$ for both $* = S, L$. We will call all Morse sets that are not attractors* unstable Morse sets.

Note that the minimality of the attractor in the partial order implies that

- every forward path starting in an attractor remains in the attractor;
- there is a forward path from any Morse set to some attractor.

Theorem 5.5. *Consider a network $\boldsymbol{RN}$ with associated multivalued maps $\mathcal{F}^S(\omega^S)$ and $\mathcal{F}^L(\Omega(\omega^S))$, and associated Morse decompositions MD^S and MD^L. Then the order preserving map $\phi : \mathsf{MD}^S \to \mathsf{MD}^L$ restricted to the sets of attractors is a surjection*

$$\phi : \mathcal{A}^S \xrightarrow{onto} \mathcal{A}^L.$$

Proof. Let $A^S \in \mathcal{A}^S$ be an attractor in MD^S. Since A^S is a strongly connected subgraph, for any $v, v' \in A^S$ there exists a path $v \to \cdots \to v'$ in the state transition graph of $\mathcal{F}^S$. Let $w := \Psi(v)$ and $w' := \Psi(v')$. By Corollary C.3, there is then a path from w to w' in the state transition graph of $\mathcal{F}^L$. Let

$$U := \{w' \in \mathcal{V}^L \mid \text{ there is a path from some } w \in \Psi(A^S) \text{ to } w'\},$$

and let A be the maximal strongly connected subgraph containing U. Clearly, A is an attractor

in $\mathcal{A}^L$. It follows from the definition of ϕ in Theorem 5.3 that

$$\phi(A^S) = A.$$

We now need to show that the restriction of ϕ on $\mathcal{A}^S$ is a surjection.

Consider an attractor $A^L \in \mathcal{A}^L$. If $u \in A^L$ such that $(g^L)^{-1}(u) \notin \mathcal{K}_N^L$, by Corollary C.5 there is a path from u to u' with $u' = g^L(\kappa)$ for some $\kappa \in \mathcal{K}_N^L$. Since forward paths starting at $u \in A^L$ remain in A^L by definition of the attractor, we conclude that A^L must contain the vertex u'. Let $\Psi^{-1}(u') =: v' \in \mathcal{V}^S$. There must be an attractor A_1^S such that there is a path from v' to any $v \in A_1^S$ in the state transition graph of $\mathcal{F}^S$. By Corollary C.3 any such path can be lifted to a path from u' to $w := \Psi(v)$ in the state transition graph of $\mathcal{F}^L$. By construction of the map ϕ, $w \in \phi(A_1^S)$. However, since any attractor must contain all of its forward paths and $u' \in A^L$, this implies that $w \in A^L$. Since $v \in A_1^S$ was arbitrary and there is a $w = \Psi(v)$ for each $v \in A_1^S$, we have that $A^L \supseteq \phi(A_1^S)$. Since $\phi(A_1^S)$ is maximal by definition, $A^L = \phi(A_1^S)$. ∎

Theorem 5.5 says the the long term behavior of $\mathcal{F}^S$ captures all long term behavior of the richer map $\mathcal{F}^L$ at the corresponding parameters for networks with no negative self-regulation. Attractors of $\mathcal{F}^S$ can merge under this correspondence Ω but the number of attractors cannot increase when employing the class of models $\mathcal{F}^L$. The assumption that **RN** does not contain a negative self-loop is essential since the result is not true when there is negative self-regulation [28], because then fixed points may appear in domains $\kappa \in \mathcal{K}^L \setminus \mathcal{K}_N^L$.

We show a stronger relationship between the specific types of attractors of $\mathcal{F}^S$ and $\mathcal{F}^L$.

Definition 5.6. *Define* $\mathsf{FP}^* \subset \mathcal{A}^*$ *to be the set of attractors that consist of a single vertex* $v \in \mathcal{V}^*$. *We call* $A \in \mathsf{FP}^*$ *a* fixed point.

Theorem 5.7. *Consider a network* **RN** *with associated nearest neighbor multivalued maps* $\mathcal{F}^S(\omega^S)$ *and* $\mathcal{F}^L(\Omega(\omega^S))$. *Let* FP^S *and* FP^L *be the associated sets of fixed points. Then the restriction of* ϕ *to* FP^S *is a bijection*

$$\phi : \mathsf{FP}^S \to \mathsf{FP}^L.$$

Proof. Consider $w \in \mathsf{FP}^L$. Then by Corollary C.5 the domain $\kappa := (g^L)^{-1}(w)$ must be a domain $\kappa \in \mathcal{K}_N^L$ and, therefore, $v := \Psi^{-1}(w) \in \mathcal{V}^S$ is well-defined. Then it follows from Corollary C.3 that since there are no paths that exit w in $\mathcal{V}^L$, there are no exiting paths from v in $\mathcal{V}^S$. Therefore $v \in \mathsf{FP}^S$. ∎

We now present important examples that show that these results cannot be strengthened in several natural directions. We will show that

1. the map $\phi : \mathsf{MD}^S(\omega) \to \mathsf{MD}^L(\Omega(\omega))$ does not have to be surjective; see Lemma 6.1;
2. the map $\phi : \mathsf{MD}^S(\omega) \to \mathsf{MD}^L(\Omega(\omega))$ does not have to be injective; see Lemma 6.4;
3. the map $\phi : \mathcal{A}^S(\omega) \to \mathcal{A}^L(\Omega(\omega))$ does not have to be injective; see Lemma 6.5.

6. Examples.

We will now present a series of examples illustrating differences which can arise between $\mathcal{F}^S$ and $\mathcal{F}^L$. In all of the following examples, we suppose that parameters $\gamma_i^S = \gamma_i^L = 1$ for all $i \in \{1, \ldots, N\}$. In addition, in several figures we will show the Morse graphs as an abstract representation of Morse decompositions; see Definition 2.6.

We will be comparing the Morse decomposition of the parameterized S-system to the Morse decomposition of the parameterized L-system under the canonical parameter map Ω. Each equivalence class $\omega \in \mathcal{Z}^S$ or $\Omega(\omega) \in \mathcal{Z}^L$ is represented by a collection of inequalities. The inequalities determine the order of the thresholds and the images of maps D^S and D^L_N for every state. For example, suppose we have the nodes $i, j, k, m, n \in \mathbf{RN}$, with i, j additive, positive inputs to node k, and m, n the outputs of k. Assume that i and j only affect node k, so that they each have two states, 0 and 1. Since k has two output thresholds, it has three states, 0, 1, and 2. Suppose further that we have the inequality description

$$l_{k,i} + l_{k,j} < \theta_{m,k} < u_{k,i} + l_{k,j} < \theta_{n,k} < l_{k,i} + u_{k,j} < u_{k,i} + u_{k,j} \tag{13}$$

for the node k. This implies that the threshold order of k is

$$O_k = \{m < n\}$$

and that the kth component of the map D^S is

$$00 \mapsto 0, \quad 10 \mapsto 1, \quad 01 \mapsto 2, \quad 11 \mapsto 2.$$

When i, j are in their 0 states, they are contributing a low value l, and when they are in their higher 1 states, they are contributing a high value u to node k. A complete description of $\omega \in \mathcal{Z}^S$ includes an inequality description like (13) for every node $k \in \mathbf{RN}$. A more complete explanation can be found in [16].

In this section all the explicit examples of differential equations will be those of an S-system. We therefore drop the superscript S on functions σ^S, and will use σ^- and σ^+ to denote piecewise constant nonlinearities that correspond to negative versus positive regulation in $\mathbf{RN}$, respectively. See Figure 1 (left) for an example of σ^-. In σ^+, using the notation in Figure 1 (left), the lower value $l_{y,x}$ is attained at $x < \theta_{y,x}$ and the higher value $u_{y,x}$ is attained for $x > \theta_{y,x}$.

Lemma 6.1. *The map $\phi : \mathsf{MD}^S \to \mathsf{MD}^L$ is, in general, not surjective.*

Proof. Consider the network shown in Figure 2, with the system of equations

$$\dot{x} = -\gamma_x x + \sigma^-_{x,y}(y), \qquad \dot{y} = -\gamma_y y + \sigma^-_{y,x}(x) \tag{14}$$

and $\omega \in \mathcal{Z}^S$ satisfying

$$l_{x,y} < \theta_{y,x} < u_{x,y}, \qquad l_{y,x} < \theta_{x,y} < u_{y,x}. \tag{15}$$

The corresponding graphs of $\mathcal{F}^S(\omega)$ and $\mathcal{F}^L(\Omega(\omega))$ are shown in Figure 7, along with the corresponding Morse graphs. It is clear that there cannot exist a surjective map from MD^S to MD^L, since MD^L has an extra Morse set. ∎

In Figure 7, the nodes in the Morse graphs labeled FP correspond to Morse sets that represent states with self-loops in the state transition graph. The Morse node labeled FC corresponds to an unstable Morse set composed of all of the nodes in the strongly connected

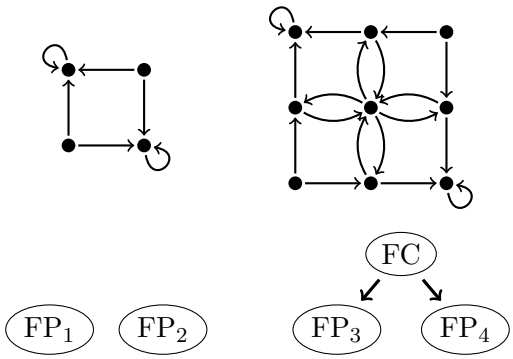

Figure 7. *The corresponding $\mathcal{F}^S(\omega)$ (top left) and $\mathcal{F}^L(\Omega(\omega))$ (top right) state transition graphs of the bistable example network under a canonical map. Also shown are the Morse graphs of $\mathcal{F}^S(\omega)$ (bottom left) and $\mathcal{F}^L(\Omega(\omega))$ (bottom right).*

four-leaf clover structure in the middle of the state transition graph. We call it *unstable* since it has paths to the upper left and lower right states, that correspond to Morse sets labeled FP. Since it is composed of more than one node this Morse set is consistent with cyclic behavior in the state transition graph. Since there is cyclic behavior for all (both) variables of the system, we will call this type of Morse set a "full cycle," or FC. When there is a Morse set with cyclic behavior in a subset of all variables, we will label it XC.

Though Corollary C.3 does guarantee that each path in the graph of $\mathcal{F}^S$ has a corresponding path in the graph of $\mathcal{F}^L$, the converse is not necessarily true. This insight is key to understanding the limits on the relationship induced by the map ϕ. To illustrate this fact, we will construct the examples in this section in multiple steps. We first start from simple two dimensional networks and then successively embed this example into successively more complicated examples, ending up with five dimensional networks. The lower dimensional examples establish how paths can exist in the graph of $\mathcal{F}^L$ that have no correlate in $\mathcal{F}^S$.

First consider the (partial) network with nodes y and z and single edge $z \dashv y$ with $l_{y,z} < \theta_{*,y} < u_{y,z}$, where $\theta_{*,y}$ is an unspecified threshold of y, and suppose that $\dot{z} < 0$. Notice that this is only part of a network in the sense that we would need at least one other interaction in order to define the threshold of y. This will be resolved when we embed this interaction into a three dimensional network. The parameterized S-system state transition graph is shown in Figure 8 on the left, and the one for the parameterized L-system on the right. Notice that paths between v_i and v_j that exist in the parameterized S-system graph map to paths between $\tilde{v}_i := \Psi(v_i)$ and $\tilde{v}_j := \Psi(v_j)$ with intermediate nodes corresponding to $(N-1)$-cells (see Lemma C.2). However, there is now a path from $\tilde{v}_3$ to $\tilde{v}_2$ which does not contain $\tilde{v}_1$, shown in cyan. The structure of the graph shown in Figure 8 on the right will play a key role in all later examples. We will embed this structure into higher dimensional state transition graphs.

Lemma 6.2. *Consider $\omega^S \in \mathcal{Z}^S$ and the nearest neighbor multivalued maps $\mathcal{F}^S(\omega^S)$ and $\mathcal{F}^L(\Omega(\omega^S))$. A path from $\Psi(v_i)$ to $\Psi(v_j)$ in the graph of $\mathcal{F}^L(\Omega(\omega))$ does not guarantee the existence of a path from v_i to v_j in the graph of $\mathcal{F}^S(\omega)$.*

Figure 8. *The fundamental structures of $\mathcal{F}^S(\omega)$, are shown left, and $\mathcal{F}^L(\Omega(\omega))$, are shown right, where $\tilde{v}_i := \Psi(v_i)$. Note the path from $\tilde{v}_3$ to $\tilde{v}_2$, shown in cyan, does not contain $\tilde{v}_1$. This structure will be embedded in all later examples.*

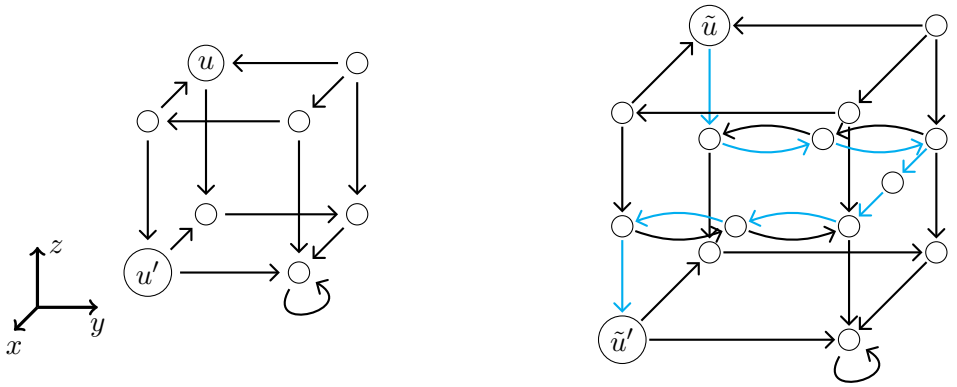

Figure 9. *Left: $\mathcal{F}^S(\omega)$, where ω satisfies (16). Notice that there is no path from u to u'. Right: A partial depiction of $\mathcal{F}^L(\Omega(\omega))$, where only some nodes are shown, and $\tilde{u} := \Psi(u)$. A path now exists from $\tilde{u}$ to $\tilde{u}'$, shown in cyan. There is one FP Morse set in each system, denoted by a self-edge in the state transition graphs.*

Proof. We embed the previous partial network in a three dimensional network with nodes x, y, and z and edges $z \dashv y \to x \dashv z$. We choose a particular $\omega \in \mathcal{Z}^S$ given by

$$l_{y,z} < \theta_{x,y} < u_{y,z}, \qquad l_{x,y} < \theta_{z,x} < u_{x,y} \qquad l_{z,x} < u_{z,x} < \theta_{y,z}. \tag{16}$$

Then $\mathcal{F}^S(\omega)$ constructed by the wall-labeling function $\mathscr{L}^S$ (see Definition 3.5) is given in Figure 9 on the left. Notice that there does not exist a path from u to u'. Also note that the structure from Figure 8 (left) occurs both on the front face and the back face of the cube in Figure 9 (left). The corresponding $\mathcal{F}^L(\Omega(\omega))$ is shown on the right with a few nodes removed for visual clarity. The bidirectional arrows in Figure 8 (right) correspond to bidirectional arrows in Figure 9 (right) that allow us to find a path from $\tilde{u}$ to $\tilde{u}'$ in $\mathcal{F}^L(\Omega(\omega))$, where $\tilde{u} := \Psi(u)$. ∎

Note that the new path from $\tilde{u}$ to $\tilde{u}'$ in the graph of $\mathcal{F}^L(\Omega(\omega))$ does not have any effect on the set of Morse sets in the two systems; in both $\mathcal{F}^S(\omega)$ and $\mathcal{F}^L(\Omega(\omega))$ there is a unique (attracting) Morse set that consists of the state in the lower right corner of the state transition graph. As a step toward showing that new paths can have an effect on the Morse decomposition, we now embed the structure of Figure 9 into a state transition graph for a

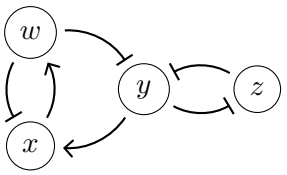

Figure 10. *The regulatory network associated with the S-system given by* (17).

four dimensional network, and proceed to explore paths from $\Psi(u)$, where $u \in A \in \mathcal{A}^S$ is a state in an attractor of a parameterized S-system.

Lemma 6.3. *Consider the network shown in Figure 10 and a corresponding S-system. There exists a parameter $\omega \in \mathcal{Z}^S$, attractor $A \in \mathcal{A}^S$, and two states $v_i \in A, v_j \notin \bigcup_{A_k \in \mathcal{A}^S} A_k$ such that there is a path from $\Psi(v_i)$ to $\Psi(v_j)$ in the graph of $\mathcal{F}^L(\Omega(\omega))$.*

Proof. Consider the network shown in Figure 10. We associate with this network the following equations:

$$\begin{aligned} \dot{x} &= -\gamma_x x + \sigma^+_{x,y}(y)\sigma^-_{x,w}(w), \\ \dot{y} &= -\gamma_y y + \sigma^-_{y,z}(z)\sigma^-_{y,w}(w), \\ \dot{z} &= -\gamma_z z + \sigma^-_{z,y}(y), \\ \dot{w} &= -\gamma_w w + \sigma^+_{w,x}(x), \end{aligned} \tag{17}$$

and consider $\omega \in \mathcal{Z}^S$ satisfying

$$\begin{aligned} l_{x,w}l_{x,y} < \begin{Bmatrix} u_{x,w}l_{x,y} \\ l_{x,w}u_{x,y} \end{Bmatrix} < \theta_{w,x} < u_{x,w}u_{x,y}, \\ l_{y,w}l_{y,z} < l_{y,w}u_{y,z} < \theta_{z,y} < u_{y,w}l_{y,z} < \theta_{x,y} < u_{y,w}u_{y,z}, \\ l_{z,y} < \theta_{y,z} < u_{z,y}, \\ l_{w,x} < \theta_{x,w} < \theta_{y,w} < u_{w,x}. \end{aligned} \tag{18}$$

The parameter (18) gives rise to the state transition graph $\mathcal{F}^S(\omega)$ shown in Figure 11, where the arrows between domains were assigned using the wall-labeling function $\mathscr{L}^S$ (see Definition 3.5). The nodes shown with square shapes are the nodes of a cyclic attractor in $\mathcal{F}^S(\omega)$, which can be verified to be an attractor by noting that there are no edges from any square to any circle, and that there is a path from every square node to every other square node. When considering the state transition graph $\mathcal{F}^L(\Omega(\omega))$, the right half of the top box in Figure 11 (corresponding to the lowest values of w) is identical to Figure 9. Therefore, as in that picture, there is a path from $\Psi(u)$ to $\Psi(u')$ in $\mathcal{F}^L$, even though there is no path from u to u'. Since u in Figure 11 is in the attractor and u' is not, this path demonstrates the lemma. ∎

The above proof is based on a network with four nodes. We do not know if such an example exists for $N = 3$, but we suspect it cannot without relaxing the constraints on our logic functions $\bar{M}_j$ (see section 2.1).

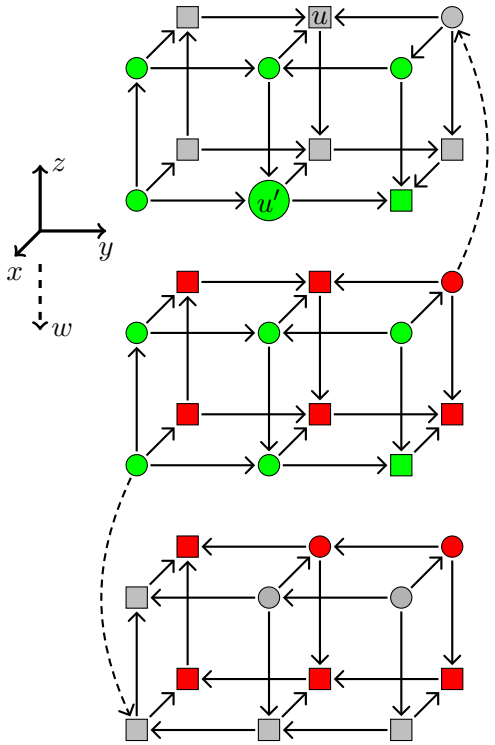

Figure 11. *$\mathcal{F}^S(\omega)$ from Lemma 6.3, with the network shown in Figure 10, S-system given by (17), and parameter ω satisfying (18). Nodes in the attractor are depicted as squares, whereas nodes not in the attractor are circles. The color of each node refers to the presence and direction of outgoing edges in the w direction. Green refers to an edge in the $+w$ direction, red refers to an edge in the $-w$ direction, and gray means there is no edge. Two example edges are shown as dashed arrows. The right half of the top box (corresponding to the lowest values of w) is identical to Figure 9, and so an escape path from u to u' exists in $\mathcal{F}^L(\Omega(\omega))$ as it did previously.*

Lemma 6.4. *The order-preserving map $\phi : \mathsf{MD}^S \to \mathsf{MD}^L$ is not necessarily injective.*

Proof. To prove the result, it is sufficient to find a network and parameters in which there exist two paths u to u' and u' to u in $\mathcal{F}^L(\Omega(\omega))$, where $\Psi^{-1}(u) \in A$ and $\Psi^{-1}(u') \in B$ for some Morse sets $A, B \in \mathsf{MD}^S$ with $A \neq B$. In this way, two distinct Morse sets in the graph of $\mathcal{F}^S(\omega)$ will merge into one strongly connected component of $\mathcal{F}^L(\Omega(\omega))$. To do so, we take the previous example network and embed it into in a five dimensional network (shown in Figure 12 (left)), with the system of equations given by

$$
\begin{aligned}
\dot{x} &= -\gamma_x x + \sigma^+_{x,y}(y)\sigma^-_{x,w}(w),\\
\dot{y} &= -\gamma_y y + \sigma^+_{y,v}(v)\sigma^-_{y,w}(w)\sigma^-_{y,z}(z),\\
\dot{z} &= -\gamma_z z + \left[\sigma^-_{z,y}(y) + \sigma^+_{z,v}(v)\right],\\
\dot{w} &= -\gamma_w w + \sigma^-_{w,v}(v)\sigma^+_{w,x}(x),\\
\dot{v} &= -\gamma_v v + \sigma^+_{v,x}(x)\sigma^-_{v,y}(y)\sigma^-_{v,w}(w),
\end{aligned}
\tag{19}
$$

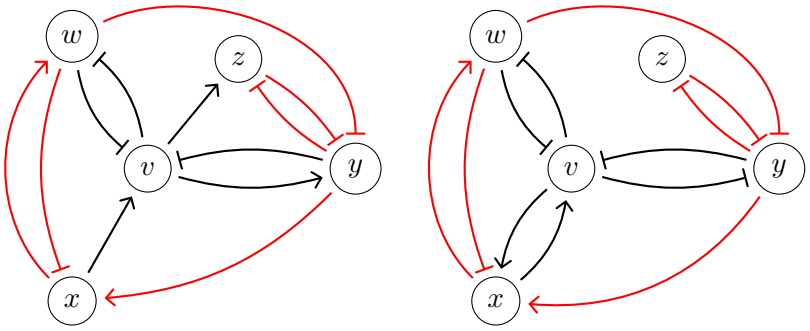

Figure 12. *Left: The five dimensional network for Lemma 6.4. Right: The five dimensional network for Lemma 6.5. In both cases, the embedded four dimensional network is shown in red.*

and $\omega \in \mathcal{Z}^S$ satisfying

$$\begin{Bmatrix} l_{x,y}l_{x,w} \\ l_{x,y}u_{x,w} \\ u_{x,y}l_{x,w} \end{Bmatrix} < \theta_{w,x} < \theta_{v,x} < u_{x,y}u_{x,w},$$

$$\begin{Bmatrix} l_{y,v}l_{y,w}l_{y,z} \\ l_{y,v}l_{y,w}u_{y,z} \end{Bmatrix} < \theta_{z,y} < l_{y,v}u_{y,w}l_{y,z} < \theta_{v,y} < \theta_{x,y} < \begin{Bmatrix} l_{y,v}u_{y,w}u_{y,z} \\ u_{y,v}u_{y,w}u_{y,z} \\ u_{y,v}l_{y,w}l_{y,z} \\ u_{y,v}l_{y,w}u_{y,z} \\ u_{y,v}u_{y,w}u_{y,z} \end{Bmatrix},$$

$$l_{z,y} + l_{z,v} < \theta_{y,z} < \begin{Bmatrix} l_{z,y} + u_{z,v} \\ u_{z,y} + l_{z,v} \\ u_{z,y} + u_{z,v} \end{Bmatrix}, \tag{20}$$

$$l_{w,v}l_{w,x} < \begin{Bmatrix} u_{w,v}l_{w,x} \\ l_{w,v}u_{w,x} \end{Bmatrix} < \theta_{v,w} < \theta_{x,w} < \theta_{y,w} < u_{w,v}u_{w,x},$$

$$l_{v,x}l_{v,y}l_{v,w} < \begin{Bmatrix} l_{v,x}l_{v,y}u_{v,w} \\ l_{v,x}u_{v,y}l_{v,w} \\ u_{v,x}l_{v,y}l_{v,w} \end{Bmatrix} < \begin{Bmatrix} l_{v,x}u_{v,y}u_{v,w} \\ u_{v,x}l_{v,y}u_{v,w} \\ u_{v,x}u_{v,y}l_{v,w} \end{Bmatrix} < \theta_{w,v} < \theta_{x,v} < \theta_{y,v} < u_{v,x}u_{v,y}u_{v,w}.$$

The full state transition graph of $\mathcal{F}^S(\omega)$ is quite extensive, so we offer a schematic in Figure 13. Each square corresponds to a three dimensional subset of nodes corresponding to domains κ that differ in coordinates x, y, and z. The coordinates v, w of domains κ are represented explicitly in the two dimensional schematic. The square in cyan is shown in greater detail in Figure 14. Arrows between squares show the existence of gradient flow between sets of domains κ in the given direction. This means that there are no paths in the direction opposite the arrow between any pair of nodes that represent domains κ, κ' that share the same x, y, z coordinates. The dark blue rectangles labeled XC_1 and XC_2 indicate the existence of Morse sets in the five dimensional state transition subgraph of $\mathcal{F}^S(\omega)$ that is represented by the boxes that the blue rectangles overlap. XC_2 is an unstable Morse set, because there is a path from a node in XC_2 to XC_1, which can be seen in Figure 17 in the appendix where we

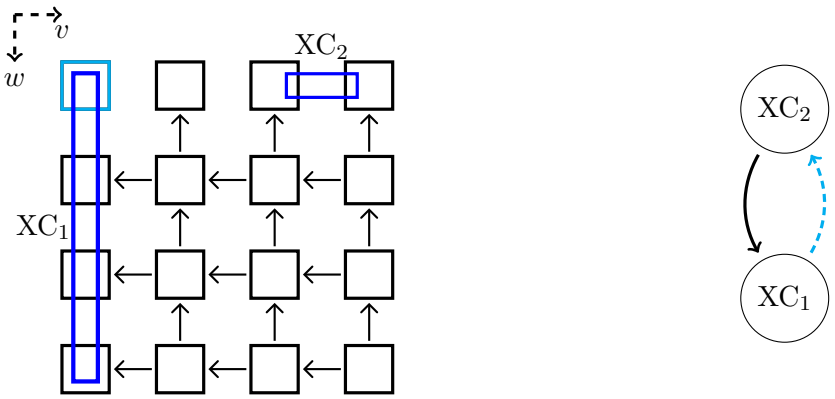

Figure 13. *Left: A general schematic of $\mathcal{F}^S(\omega)$ from Lemma 6.4. Each square corresponds to a three dimensional subset of nodes, with coordinates differing in x, y, and z only. The square in cyan is shown in greater detail in Figure 14. Arrows between squares refer to gradient flow in the given direction. The dark blue rectangles labeled XC_1 and XC_2 represent Morse sets (see the text for a full explanation). In $\mathcal{F}^L(\Omega(\omega))$, there is a new path in the cyan box which connects XC_1 to XC_2. The full left column and top row are provided in Figures 16 and 17 (left), respectively. Right: The corresponding (partial) Morse graph. The cyan edge is added only in $\mathcal{F}^L(\Omega(\omega))$, merging XC_1 and XC_2 into one strongly connected component, showing that ϕ, in general, is not injective between the Morse decompositions.*

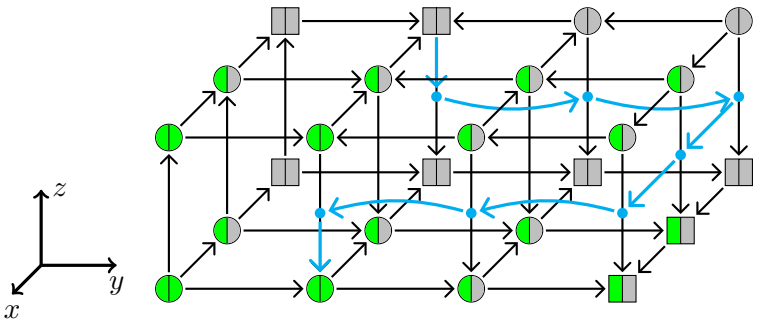

Figure 14. *The full set of nodes which correspond to the upper left cyan square in both Figures 13 and 15. Nodes in XC_1 are denoted as squares; all other nodes are circles. The cyan path exists in $\mathcal{F}^L(\Omega(\omega))$ from a node in XC_1 to a node not in it. This path makes use of the same structure as the previous examples. The color of each node refers to the outgoing arrows in the w and v directions. The left half of each node corresponds to w and the right half to v. Green means there is an edge from the node to the next corresponding node in the $+$ direction. Gray means no outgoing edge in the corresponding direction. There are no edges in the $-$ direction, since this graph represents the lowest states of the v and w directions.*

exhibit the full state transition graph. The Morse graph MG^S is shown in Figure 13 (right) with only the black arrow.

In $\mathcal{F}^L(\Omega(\omega))$, there is a new path in the cyan box which connects XC_1 to XC_2, as depicted in Figure 14. This escape path joins the boxes associated with XC_1 and XC_2, leading to the dashed cyan arrow shown in Figure 13 (right), which is not present for $\mathcal{F}^S(\omega)$. This backward path in $\mathcal{F}^L(\Omega(\omega))$ means that the associated Morse decomposition consists of a single node representing one large cycle, and therefore the map ϕ takes both Morse sets of $\mathcal{F}^S(\omega)$ to the single Morse set of $\mathcal{F}^L(\Omega(\omega))$. ■

In the previous example, both an attractor Morse set and an unstable Morse set of MD^S are mapped under ϕ onto the single attractor of MD^L. A natural question is whether two attractors of MD^S can be mapped to a single attractor in MD^L. We show that this is indeed possible.

Lemma 6.5. *The order-preserving map $\phi : \mathcal{A}^S \to \mathcal{A}^L$ restricted only to attractors is, in general, not injective.*

Proof. To show this we modify the network and parameter of the previous lemma. Consider the network in Figure 12 (right). Again, the basic structure of $\mathcal{F}^S(\omega)$ with ω from (18) as shown in Figure 11 will be embedded in XC_1 of the first column in the schematic Figure 15 (left). We will exhibit a path from a node $u \in \mathcal{V}^L$, where $\Psi^{-1}(u) \in A$ for some $A \in \mathcal{A}^S$ to a node $u' \in \mathcal{V}^L$, where $\Psi^{-1}(u') \in B$ for an attractor $B \neq A$. To do so, we endow the network shown in Figure 12 right with an S-system

$$
\begin{aligned}
\dot{x} &= -\gamma_x x + \left[\sigma^+_{xy}(y) + \sigma^+_{xv}(v)\right] \sigma^-_{xw}(w),\\
\dot{y} &= -\gamma_y y + \sigma^-_{yz}(z)\sigma^-_{yw}(w)\sigma^-_{yv}(v),\\
\dot{z} &= -\gamma_z z + \sigma^-_{zy}(y),\\
\dot{w} &= -\gamma_w w + \sigma^+_{wx}(x)\sigma^-_{wv}(v),\\
\dot{v} &= -\gamma_v v + \sigma^+_{vx}(x)\sigma^-_{vy}(y)\sigma^-_{vw}(w),
\end{aligned} \tag{21}
$$

and we consider $\omega \in \mathcal{Z}^S$ satisfying

$$
(l_{x,y}+l_{x,v})l_{x,w} < \left\{\begin{matrix}(u_{x,y}+l_{x,v})l_{x,w}\\(l_{x,y}+u_{x,v})l_{x,w}\\(l_{x,y}+l_{x,v})u_{x,w}\\(l_{x,y}+u_{x,v})u_{x,w}\end{matrix}\right\} < \theta_{w,x} < \theta_{v,x} < \left\{\begin{matrix}(u_{x,y}+l_{x,v})u_{x,w}\\(u_{x,y}+u_{x,v})l_{x,w}\end{matrix}\right\} < (u_{x,y}+u_{x,v})u_{x,w}, \tag{22}
$$

$$
l_{y,z}l_{y,w}l_{y,v} < \left\{\begin{matrix}u_{y,z}l_{y,w}l_{y,v}\\l_{y,z}u_{y,w}l_{y,v}\\l_{y,z}l_{y,w}u_{y,v}\\u_{y,z}u_{y,w}l_{y,v}\\u_{y,z}l_{y,w}u_{y,v}\end{matrix}\right\} < \theta_{z,y} < l_{y,z}u_{y,w}u_{y,v} < \theta_{v,y} < \theta_{x,y} < u_{y,z}u_{y,w}u_{y,v}, \tag{23}
$$

$$
l_{z,y} < \theta_{y,z} < u_{z,y}, \tag{24}
$$

$$
l_{w,v}l_{w,x} < \left\{\begin{matrix}u_{w,v}l_{w,x}\\l_{w,v}u_{w,x}\end{matrix}\right\} < \theta_{v,w} < \theta_{x,w} < \theta_{y,w} < u_{w,v}u_{w,x}, \tag{25}
$$

$$
l_{v,x}l_{v,y}l_{v,w} < \left\{\begin{matrix}l_{v,x}l_{v,y}u_{v,w}\\l_{v,x}u_{v,y}l_{v,w}\\u_{v,x}l_{v,y}l_{v,w}\end{matrix}\right\} < \left\{\begin{matrix}l_{v,x}u_{v,y}u_{v,w}\\u_{v,x}l_{v,y}u_{v,w}\\u_{v,x}u_{v,y}l_{v,w}\end{matrix}\right\} < \theta_{w,v} < \theta_{z,v} < \theta_{y,v} < u_{v,x}u_{v,y}u_{v,w}. \tag{26}
$$

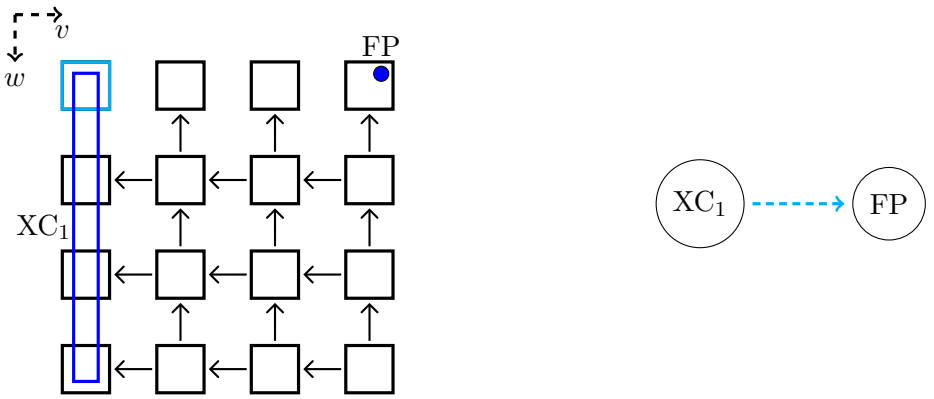

Figure 15. *Left: Similar to Figure 13, a general schematic of $\mathcal{F}^S(\omega)$ from Lemma 6.5. Each square corresponds to a three dimensional subset of nodes, with coordinates differing in x, y, and z only. Arrows between squares refer to gradient flow in the given direction. The square in cyan is shown in greater detail in Figure 14. In $\mathcal{F}^L(\Omega(\omega))$, there is a new path in the cyan box which connects XC_1 to FP. The full left column and top row are provided in Figures 16 and 17, respectively. Right: The corresponding (partial) Morse graph. The cyan edge is added only in $\mathcal{F}^L(\Omega(\omega))$, showing that ϕ cannot be made injective even when constrained to attractors. In effect, XC_1 loses stability in $\mathcal{F}^L(\Omega(\omega))$.*

A schematic of $\mathcal{F}^S(\omega)$ is shown in Figure 15. In the parameterized S-system there are two attractors, XC_1 which is the same as in the previous example, and a new attractor, denoted FP. The escape path depicted in Figure 14 is still present in the cyan box at the upper left in $\mathcal{F}^L(\Omega(\omega))$. This escape path now connects the boxes associated with XC_1 to the fixed point FP. It follows that in MD^L, the set of nodes $\{\Psi(v) \mid v \in \mathrm{XC}_1\}$ does not belong to an attracting cycle, and the only attractor is FP. Therefore ϕ cannot be injective even when confined to the set of attractors. ∎

Remark 6.6. The complete graphs of $\mathcal{F}^S(\omega)$ and $\mathcal{F}^L(\Omega(\omega))$ of the previous two lemmas are large and do not contribute greatly to understanding on a first reading. However, the complete set of nodes corresponding to the left column and top row are included in Figures 16 and 17. We do not include views into other three dimensional subgraphs, since there is gradient flow between them in the v or w directions, and so there are no other attractor Morse sets within them.

7. Discussion. Switching systems (S-systems in this paper) were proposed as a platform for modeling continuous time processes in gene regulation. The underlying assumption of these models is that a regulatory genetic network executes a Boolean function, but that this execution is embedded in a continuous flow of time that leads to a system of equations with discontinuous right-hand sides. One of the key advantages of the class of S-systems is that they provide a means to combinatorialize the dynamics of the ODE system in terms of state transition graphs. These provide incomplete [24, 23, 18] but important information about the dynamics. In our description this information is captured in a Morse graph [37, 16]. Morse graphs provide information on the number and type of attractors present.

There has been a lot of discussion about the technical challenges switching systems present and whether and how these models represent the dynamics of nearby perturbed continuous

models. Systems of ODEs similar to the class of L-systems have been studied as continuous perturbations of the class of S-systems [28, 22]. In this interpretation, the interval $[\vartheta^-_{j,i}, \vartheta^+_{j,i}]$ in the definition of $\sigma^L_{j,i}$ contains the threshold $\theta_{j,i}$ of $\sigma^S_{j,i}$, and has length ϵ, a small number. Then with the same values $l^L_{j,i} = l^S_{j,i}$, and $u^L_{j,i} = u^S_{j,i}$, the function $\sigma^L_{j,i}$ is a small C^0 perturbation of $\sigma^S_{j,i}$. A challenge is to characterize how the dynamics of such a nearby L-system reflects the dynamics of the similarly parameterized S-system. This is a difficult question in the ODE setting, where the emphasis is on individual trajectories. In this paper we address this question from a perspective of global dynamics, where we compare the Morse graphs associated with $\mathcal{F}^S(\omega)$ and $\mathcal{F}^L(\Omega(\omega))$. Furthermore, we do not require that the intervals $[\vartheta^-_{j,i}, \vartheta^+_{j,i}]$ are small; this is replaced by the requirement that $[\vartheta^-_{j,i}, \vartheta^+_{j,i}] \cap [\vartheta^-_{k,i}, \vartheta^+_{k,i}] = \emptyset$.

Viewing an L-system parameterized by $\Omega(\omega)$ to be a perturbation of an S-system parameterized by ω, we study the natural question of how the Morse graph of the perturbation MG^L relates to the original MG^S for a class of regulatory networks with no negative self-regulation. We show that there is a surjection from the set of attractors in the Morse graph of a parameterized S-system to the set of attractors of the corresponding parameterized L-system, and that this surjection is a bijection on the set of fixed-point attractors. Therefore no new stable behavior can be introduced by a perturbation to this type of continuous system. Thus the parameterized S-system contains essential information about the attractors of the continuous systems, although attractors may merge under such a perturbation.

As important as these results are, our constructed examples of systems show that stronger relationships than those exhibited do not exist. First, we construct an example that shows that a parameterized L-system can have more nonattractor Morse sets than the corresponding parameterized S-system. Second, we construct an L-system that combines two attractors of the S-system into a single attractor of the L-system. As a consequence of these results, one way one could hope to strengthen the results about the correspondence between the Morse graphs of the switching system and its continuous perturbations, represented by L-systems, is to refine the definition of the state transition graph for the L-system. Whether such a refinement would provide a closer correspondence between Morse graphs is currently an open question.

Appendix A. Proof of Theorem 3.8.

Proof. Let κ and κ' be two domains with corresponding states $s_1 := g^S(\kappa)$ and $s_2 := g^S(\kappa')$, using the notation of Definition 2.4. Note that the target state of κ is given by

$$t_1 := D^S(s_1) = G^S \circ \Gamma^{-1}\Lambda^S(\kappa),$$

using (8).

First suppose that $s_1 = s_2 = t_1$, as in part (a) of Definition 2.3 of a multivalued map. This is true if and only if $\Gamma^{-1}\Lambda^S(\kappa) \in \kappa$, which is equivalent to κ being an attracting domain, which is exactly part (a) of Definition 3.6.

Now we consider parts (a) and (b) of Definition 2.4. Note that two domains κ and κ' are adjacent if and only if the corresponding states s_1 and s_2 are adjacent. So presume that κ and κ' share a face τ, which means s_1 and s_2 are adjacent. Let $\theta_{j,i} = \pi_i(\tau)$ be the threshold at the face, and assume without loss of generality that τ is a right face of κ and a left face of κ', so that $\operatorname{sgn}(\tau, \kappa) = -1$, $\operatorname{sgn}(\tau, \kappa') = 1$. By the definition of g^S, this means that $s_{1,i} < s_{2,i}$.

Assume first that $s_2 \in \mathcal{F}^S(s_1)$ so that $\mathscr{L}^S((\tau,\kappa)) = -1$, $\mathscr{L}^S((\tau,\kappa')) = 1$. Since $\operatorname{sgn}(\tau,\kappa) = \mathscr{L}^S((\tau,\kappa)) = -1$ by assumption, we have

$$\begin{aligned} &\operatorname{sgn}(\Lambda_i^S(\kappa)/\gamma_i^S - \theta_{j,i}) = 1 \\ \Rightarrow\ &\Lambda_i^S(\kappa)/\gamma_i^S > \theta_{j,i} > \pi_i(\operatorname{int}\kappa). \end{aligned}$$

Since $s_{1,i} = \pi_i(g^S(\kappa)) = G_i^S(x_{1,i})$ for arbitrary $x_{1,i} \in \pi_i(\operatorname{int}\kappa)$, we have that

$$s_{1,i} = G_i^S(x_{1,i}) < G_i^S(\Lambda_i^S(\kappa)/\gamma_i^S) = t_{1,i}.$$

The statements $s_{1,i} < s_{2,i}$ and $s_{1,i} < t_{1,i}$ then verify Definition 2.4(a).

In the reverse direction, we have already proved that $s_{1,i} < s_{2,i}$ and $s_{1,i} < t_{1,i}$ imply $\mathscr{L}^S((\tau,\kappa)) = -1$, since all statements were equivalencies. We show that $\mathscr{L}^S((\tau,\kappa')) = 1$ by way of contradiction. Suppose $\mathscr{L}^S((\tau,\kappa')) = -1$. Then

$$\Lambda_i^S(\kappa')/\gamma_i^S < \theta_{j,i},$$

which implies that x_i is increasing below $\theta_{j,i}$ and decreasing above $\theta_{j,i}$. This means that the ith component of the target point changes between κ and κ', and these domains only differ in the ith coordinate. This implies that the node i of the network **RN** is regulating itself; the fact that it is negative self-regulation follows from the signs of the vector field in κ and κ' and the fact that $\pi_i(\operatorname{int}\kappa) < \pi_i(\operatorname{int}\kappa')$. Since we assume that **RN** has no negative self-regulation, it must be that $\mathscr{L}^S((\tau,\kappa')) = 1$, as desired.

We have shown that if there are two adjacent domains κ on the left and κ' on the right and $s_2 \in \mathcal{F}^S(s_1)$ according to Definition 3.6(b), this is equivalent to condition (b).1 in Definition 2.4. We leave it to the reader to show in a similar fashion that if $s_{2,i} > s_{1,i}$ and $s_{2,i} > t_{2,i}$ (interchanging indices 1 and 2) then the Definition 2.4(b) is equivalent to $s_1 \in \mathcal{F}^S(s_2)$ under the same domain adjacency conditions. ∎

Appendix B. Proof of Theorem 3.13. The main result in this section is Theorem B.2, from which the proof of Theorem 3.13 follows.

For any ℓ-cell $\zeta \in \mathbb{R}^N$, $\zeta = \prod_{i=1}^N [\varphi_i, \varphi_i']$ with $0 \le \ell \le N$ recall from Definition 3.1 that

$$ND(\zeta) := \{j \mid \varphi \neq \varphi'\}$$

is the set of nondegenerate indices, where $|ND(\zeta)| = \ell$. Let $ND^c(\zeta) := \{1,\dots,N\} \setminus ND(\zeta)$ be the complement of $ND(\zeta)$.

Theorem B.1. *Let $z^L \in Z^L$ be a regular parameter for a parameterized L-system, and let $\zeta = \prod_{i=1}^N [\varphi_i, \varphi_i']$ be an ℓ-cell in $\mathbb{R}^N$ with $0 \le \ell < N$. For $k \in ND(\zeta)$ let $W_k := \zeta \cap \{x \mid x_k = \varphi_k\}$ and let $W_k' := \zeta \cap \{x \mid x_k = \varphi_k'\}$. In the case where $\varphi_k' = \infty$, choose an arbitrary point p with $p_k > \varphi_k$ and set $W_k' := \zeta \cap \{x \mid x_k = p_k\}$. Then for any $j \in ND^c(\zeta)$*

1. *$\dot{x}_j > 0$ on $W_k \cup W_k'$ implies $\dot{x}_j > 0$ everywhere in ζ;*
2. *$\dot{x}_j < 0$ on $W_k \cup W_k'$ implies $\dot{x}_j < 0$ everywhere in ζ.*

Proof. Let ζ be an ℓ-cell with $0 \le \ell < N$ and let $k \in ND(\zeta)$. Define W_k and W_k' as in the Theorem. Let $j \in ND^c(\zeta)$; then $\zeta \subseteq \{x \mid x_j = \varphi_j\}$ for some threshold φ_j. Define

$$H_j(x) := \Lambda_j(x) - \gamma_j \varphi_j$$

to be the right-hand side of the equation for $\dot{x}_j = H_j(x)$ on ζ. Assume that $\operatorname{sgn}(\dot{x}_j)$ is constant and nonzero on $W_k \cup W_k' \subset \zeta$.

Let $q \in \zeta$ be an arbitrary point. Then there exists a scalar $\alpha \geq 0$ such that $u := q - \alpha\vec{e}_k \in W_k$, where $\vec{e}_k$ is the unit vector along the kth coordinate. Let $h : [0,1] \to \zeta$ be the line segment along the kth coordinate direction that starts in W_k, passes through q, and ends in W_k':

$$h(s) = u + s(\varphi_k' - \varphi_k)\vec{e}_k,\ 0 \leq s \leq 1.$$

Note that $h(0) = u \in W_k$ and $h(1) \in W_k'$ and $h(s_1) = q$ for some $s_1 \in [0,1]$.

We consider the two cases: in the first case k has a direct regulatory effect on j and hence Λ_j depends on x_k, and in the second case when Λ_j does not depend on x_k. In the second case the derivative $\dot{x}_j = H_j(x)$ does not depend on x_k. Since the only variable that changes value along the line segment $h(s)$ is x_k, the derivative $\dot{x}_j(h(s)) = H_j(h(s))$ is constant. Since we know that $\dot{x}_j$ has the same sign everywhere on W_k it must have the same sign along $h(s)$. Since q and thus $h(s)$ was arbitrary, the same is true for any point $y \in \zeta$.

Now consider the first case. We observe that on $h(s)$, the function Λ_j is a linear function of $\sigma_{j,k}(h(s))$. This occurs because Λ_j is multiaffine in $\sigma_{j,i}$ for all $i \in \mathbf{S}(j)$, the sources of j. But all $x_i \neq x_k$ are constant on $h(s)$, so Λ only changes linearly with respect to $\sigma_{j,k}(h(s))$. We conclude that $H_j(h(s))$ is a linear function in $\sigma_{j,k}(h(s))$.

Recall that $l_{j,k} \leq \sigma_{j,k}(h(s)) \leq u_{j,k}$, and lower and upper bounds are attained at the boundaries $h(s) = \varphi_k$ and $h(s) = \varphi_k'$. Therefore

$$\min\{\sigma_{j,k}(\varphi_k), \sigma_{j,k}(\varphi_k')\} \leq \sigma_{j,k}(h(s)) \leq \max\{\sigma_{j,k}(\varphi_k), \sigma_{j,k}(\varphi_k')\}.$$

From this inequality and the linearity of H_j in $\sigma_{j,k}(h(s))$, we conclude

$$\min\{H_j(h(0)), H_j(h(1))\} \leq H_j(h(s)) \leq \max\{H_j(h(0)), H_j(h(1))\}$$

for all $s \in [0,1]$.

When $\dot{x}_j > 0$ on $W_k \cup W_k'$, then $H_j(h(0)) > 0$ and $H_j(h(1)) > 0$, which implies $H_j(h(s)) > 0$ for $0 \leq s \leq 1$. Likewise, when $\dot{x}_j < 0$ on $W_k \cup W_k'$, then $H_j(h(0)) < 0$ and $H_j(h(1)) < 0$, which implies $H_j(h(s)) < 0$ for $0 \leq s \leq 1$. Since the selection of q and hence $h(s)$ was arbitrary, we have proven that the sign of $\dot{x}_j$ on ζ is determined by its sign on $W_k \cup W_k'$. ∎

Theorem B.2. *Let z^L be a regular parameter for a parameterized L-system, and let $\zeta := \prod_{i=1}^N [\varphi_i, \varphi_i']$ be an ℓ-cell in $\mathbb{R}^N$ with $0 \leq \ell < N$. Then for all $j \in ND^c(\zeta)$ we have*

1. $\texttt{Sign}(\mathcal{C}(\zeta), j) = +1$ *implies* $\dot{x}_j > 0$ *everywhere in* ζ*;*
2. $\texttt{Sign}(\mathcal{C}(\zeta), j) = -1$ *implies* $\dot{x}_j < 0$ *everywhere in* ζ*.*

Proof. Suppose $\ell = 0$. Then $\mathcal{C}(\zeta) = \zeta$ and the proof is immediate. This is the base case for an inductive proof.

Let ζ be an ℓ-cell with $1 \leq \ell < N$ and assume that for all $(\ell-1)$-cells the theorem holds. Let $j \in ND^c(\zeta)$ be a degenerate index.

First assume that $\texttt{Sign}(\mathcal{C}(\zeta), j) = +1$. Pick any $k \in ND(\zeta)$, let $[\varphi_k, \varphi_k']$ be the corresponding nondegenerate interval, and let $W_k := \zeta \cap \{x_k = \varphi_k\}$, $W_k' := \zeta \cap \{x_k = \varphi_k'\}$. Notice that by Definition 3.1, W_k and W_k' are $(\ell-1)$-cells. Furthermore $\mathcal{C}(W_k) \subseteq \mathcal{C}(\zeta)$, and so by Definition 3.10, $\texttt{Sign}(\mathcal{C}(W_k), j) = +1$. By our inductive hypothesis, $\dot{x}_j > 0$ everywhere in

W_k. A similar argument shows that $\dot{x}_j > 0$ everywhere in W_k' as well. Then by Theorem B.1, $\dot{x}_j > 0$ everywhere in ζ.

A similar argument is used when $\texttt{Sign}(\mathcal{C}(\zeta), j) = -1$. This finishes the induction and hence the proof. ∎

Appendix C. Lemmas for section 5. In the following, we assume that constructions in the S- and L-systems come from equivalence class parameters ω^S and $\omega^L := \Omega(\omega^S)$. Figure 6 shows the illustration of the maps used im (27).

Definition C.1. *We define the bijection*

$$\beta = (g^L)^{-1} \circ \Psi \circ g^S : \mathcal{K}^S \to \mathcal{K}_N^L \tag{27}$$

and the order-preserving functions

$$\beta^-(\theta_{j,i}) = \vartheta_{j,i}^-,$$
$$\beta^+(\theta_{j,i}) = \vartheta_{j,i}^+.$$

When κ, $\kappa' \in \mathcal{K}^S$ are adjacent with shared face $\tau \subset \{x \mid x_i = \theta_{j,i}\}$, consider the domain $\eta \in \mathcal{K}_{N-1}^L$,

$$\eta = \prod_{k=1}^{i-1} \beta_k(\kappa) \times [\beta^-(\theta_{j,i}), \beta^+(\theta_{j,i})] \times \prod_{k=i+1}^{N} \beta_k(\kappa).$$

It is easy to see that

1. η shares a face with $\beta(\kappa)$, $\tau^- := \eta \cap \beta(\kappa) \subset \{x \mid x_i = \vartheta_{j,i}^-\}$;
2. η shares a face with $\beta(\kappa')$, $\tau^+ := \eta \cap \beta(\kappa') \subset \{x \mid x_i = \vartheta_{j,i}^+\}$.

In other words, η is the unique domain that lies between $\beta(\kappa)$ and $\beta(\kappa')$, and this domain is in the subset $\mathcal{K}_{N-1}^L \subset \mathcal{K}^L$.

The next lemma is the key result from which many results about the correspondence between the Morse graphs follow.

Lemma C.2. *Consider $\mathcal{F}^S(\omega^S)$ and $\mathcal{F}^L(\Omega(\omega^S))$ and two adjacent domains $\kappa, \kappa' \in \mathcal{K}^S$ with shared face $\tau \subset \{x \mid x_i = \theta_{j,i}\}$. Let $\zeta := \beta(\kappa), \zeta' := \beta(\kappa')$, $\zeta, \zeta' \in \mathcal{K}_N^L$ be the corresponding domains in $\mathcal{K}_N^L$ and let $\eta \in \mathcal{K}_{N-1}^L$ be the unique domain lying between ζ and ζ'. Let $v := g^S(\kappa), v' := g^S(\kappa')$, $v, v' \in \mathcal{V}^S$, $w := g^L(\zeta), w' := g^L(\zeta'), w, w' \in \mathcal{V}^{SL}$, and $u = g^L(\eta)$. Then $v \to v' \in \mathcal{F}^S(\omega)$ if and only if $w \to u \to w' \in \mathcal{F}^L(\Omega(\omega))$.*

Proof. We consider the case when (τ, κ) is the right wall of κ ($\text{sgn}((\tau, \kappa)) = -1$) and (τ, κ') is the left wall of κ' ($\text{sgn}((\tau, \kappa')) = +1$). A similar argument holds in the other case. Then $v' \in \mathcal{F}^S(v)$ if and only if $\mathscr{L}^S((\tau, \kappa)) = -1$ and $\mathscr{L}^S((\tau, \kappa')) = +1$, which by Definition 3.5, implies that

$$\Lambda_i^S(\kappa)/\gamma^S > \theta_{j,i}, \quad \Lambda_i^S(\kappa')/\gamma^S > \theta_{j,i}.$$

By Definition 4.5 of the correspondence Ω we know that $D^S \circ g^S(\kappa) = D_N^L \circ g^L(\zeta)$, so if $\Lambda_i^S(\kappa)/\gamma^S > \theta_{j,i}$, then

$$\Lambda_i^L(\zeta)/\gamma_i^L > \beta^+(\theta_{j,i}), \quad \Lambda_i^L(\zeta')/\gamma_i^L > \beta^+(\theta_{j,i}).$$

Then from Definition 3.10 we get $\texttt{Sign}(\mathcal{C}(\tau^-), i) = \texttt{Sign}(\mathcal{C}(\tau^+), i) = +1$. We note that τ^- is a right face of ζ and a left face of η, while τ^+ is a right face of η and a left face of ζ', by the assumptions of the lemma. With this information we can compute

$$\mathscr{L}^L((\tau^-, \zeta)) = -1 \cdot +1 = -1, \quad \mathscr{L}^L((\tau^-, \eta)) = +1 \cdot +1 = +1,$$
$$\mathscr{L}^L((\tau^+, \eta)) = -1 \cdot +1 = -1, \quad \mathscr{L}^L((\tau^+, \zeta')) = +1 \cdot +1 = +1.$$

Finally, by Definition 3.12 this is equivalent to the existence of a path $w \to u \to w'$ in $\mathcal{V}^L$. Since all the previous statements are equivalencies this finishes the proof. ∎

Corollary C.3. *Consider $\mathcal{F}^S(\omega^S)$ and $\mathcal{F}^L(\Omega(\omega^S))$. For any two $v, v' \in \mathcal{V}^S$ let $w := \Psi(v)$, $w' := \Psi(v')$. Then $v' \in (\mathcal{F}^S)^k(v)$ for some integer k (which means there is a path of length k in the graph $(\mathcal{V}^S, \mathcal{E}^S)$), if and only if $w' \in (\mathcal{F}^L)^{2k}(w)$, where every domain $\kappa_i = (g^L)^{-1}(w_i)$ belongs to $\mathcal{K}^L_N \cup \mathcal{K}^L_{N-1}$ for all nodes w_i in the path.*

Lemma C.4. *Consider a regulatory network $\boldsymbol{RN}$, a parameterized L-system with regular parameter $z^L \in Z^L$, the set of domains $\mathcal{K}^L$, and nearest neighbor multivalued map $\mathcal{F}^L$. Let $\kappa \in \mathcal{K}^L \setminus \mathcal{K}^L_N$ be a domain and let $u = g^L(\kappa)$ have k noninteger components. Then there is a state $v \in \mathcal{V}^L$ with $k-1$ noninteger components, such that*

$$v \in \mathcal{F}^L(u).$$

Proof. Let $\kappa \in \mathcal{K}^L \setminus \mathcal{K}^L_N$ with $u = g^L(\kappa)$. Then there is an index i such that $\pi_i(\kappa) = [\vartheta^-_{j,i}, \vartheta^+_{j,i}]$. Let τ^- and τ^+ be the left and right faces of κ with projection index i and so $\tau^- \subseteq \{x \mid x_i = \vartheta^-_{j,i}\}$ and $\tau^+ \subseteq \{x \mid x_i = \vartheta^+_{j,i}\}$. Note that there are two domains η^-, η^+ that are immediate neighbors of κ along the ith coordinate which satisfy

$$\pi_i(\eta^-) = [\vartheta^+_{j-1,i}, \vartheta^-_{j,i}], \qquad \pi_i(\eta^+) = [\vartheta^+_{j,i}, \vartheta^-_{j+1,i}].$$

It follows that the states

$$v^- := g^L(\eta^-) \text{ and } v^+ := g^L(\eta^+)$$

have one more integer value than u.

Let $\mathcal{C}(\tau^-)$ be a collection of corner points of τ^- and $\mathcal{C}(\tau^+)$ be a collection of corner points of τ^+. Note that there is a bijection α between these two sets and the corresponding corner points that only differ in the ith values where $\vartheta^-_{j,i}$ is replaced by $\vartheta^+_{j,i}$. Take $q \in \mathcal{C}(\tau^-)$ and assume first that $\texttt{Sign}(q, i) = +1$. This implies that $\Lambda^L_i(q)/\gamma^L_i > \vartheta^-_{j,i}$. But since at any regular parameter z^L the value

$$\Lambda^L_i(q)/\gamma^L_i \notin [\vartheta^-_{j,i}, \vartheta^+_{j,i}]$$

for any j, we conclude that also $\Lambda^L_i(q)/\gamma^L_i > \vartheta^+_{j,i}$. This in turn implies that at the corner point $\alpha(q) \in \mathcal{C}(\tau^+)$ we have $\texttt{Sign}(\alpha(q), i) = +1$. We have shown that

$$\texttt{Sign}(q, i) = +1 \quad \text{if and only if} \quad \texttt{Sign}(\alpha(q), i) = +1.$$

A similar argument shows that $\texttt{Sign}(q, i) = -1$ if and only if $\texttt{Sign}(\alpha(q), i) = -1$ as well.

Let $u = g^L(\kappa)$. From the definition of the map $\mathcal{F}^L$ we have

- if there exists at least one corner point $q \in \mathcal{C}(\tau^-)$ with $\texttt{Sign}(q,i) = -1$, then

$$v^- \in \mathcal{F}^L(u);$$

- if there exists at least one corner point $q \in \mathcal{C}(\tau^+)$ with $\texttt{Sign}(q,i) = +1$, then

$$v^+ \in \mathcal{F}^L(u).$$

Since the Sign of a single corner point can never be zero by the regularity of z^L, we conclude that either one or both of the cases hold. ∎

Corollary C.5. *Consider a regulatory network* $\boldsymbol{RN}$*, a parameterized L-system with regular parameter* $z^L \in Z^L$*, the set of domains* $\mathcal{K}^L$*, and nearest neighbor multivalued map* $\mathcal{F}^L$*. Let* $\kappa \in \mathcal{K}^L \setminus \mathcal{K}^L_N$ *be a domain and let* $u = g^L(\kappa)$ *have* k *noninteger components. Then there is a state* $v \in \mathcal{V}^{SL} \subset \mathcal{V}^L$ *with integer components such that for some* $j \geq k$

$$v \in (\mathcal{F}^L)^j(u).$$

Proof. Proof is immediate by inductively applying Lemma C.4. ∎

Appendix D. State transition graphs for the five dimensional examples. We now present full information about the paths in the proofs of Lemmas 6.4 and 6.5. The first column (Figure 16) and the first rows (Figure 17) of the schematics in Figures 13 and 15 are shown below. The rows have been rotated into columns to make them more legible, and are arranged for side-by-side comparison.

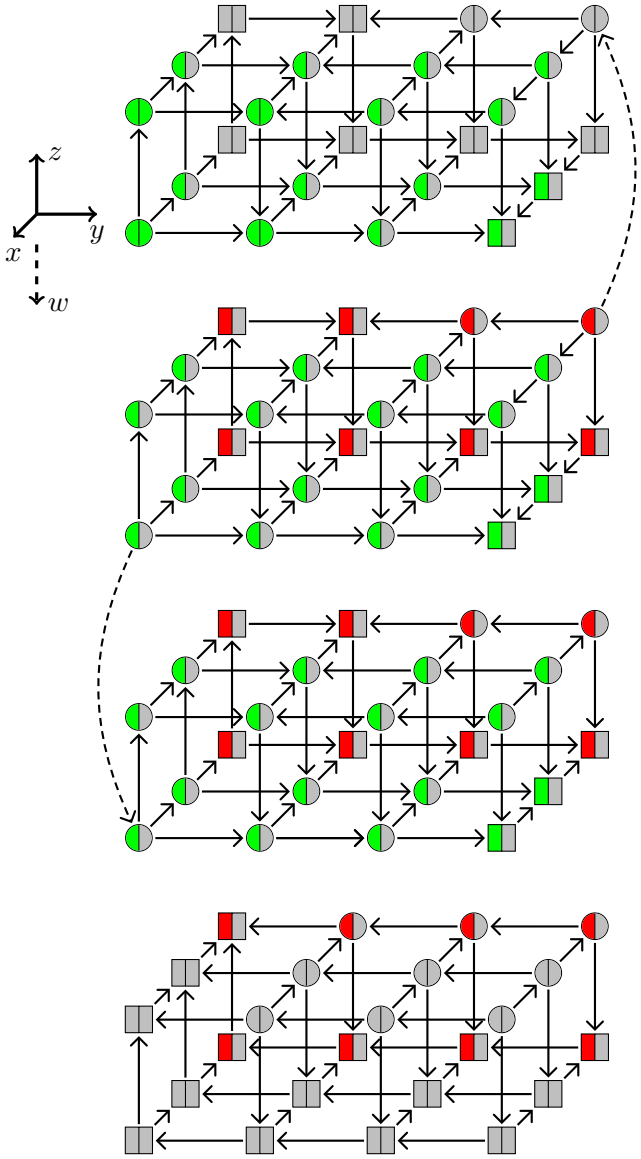

Figure 16. *The left column of both Figures 13 and 15. Our choice of networks and parameters allows us to use the same structure in $\mathcal{F}^S$ for the nodes corresponding to the lowest values of v (the top cuboid). The color of each node refers to the outgoing arrows in the v and w directions. The left half of each node corresponds to w and the right half to v. Green means there is an edge from the node to the next corresponding node in the $+$ direction, and red means there is an edge in the $-$ direction. Gray means no outgoing edge in the corresponding direction. Two example dashed arrows are shown. Nodes in XC_1 are shown as squares; all other nodes are shown as circles. The top box is the same one shown in Figure 14.*

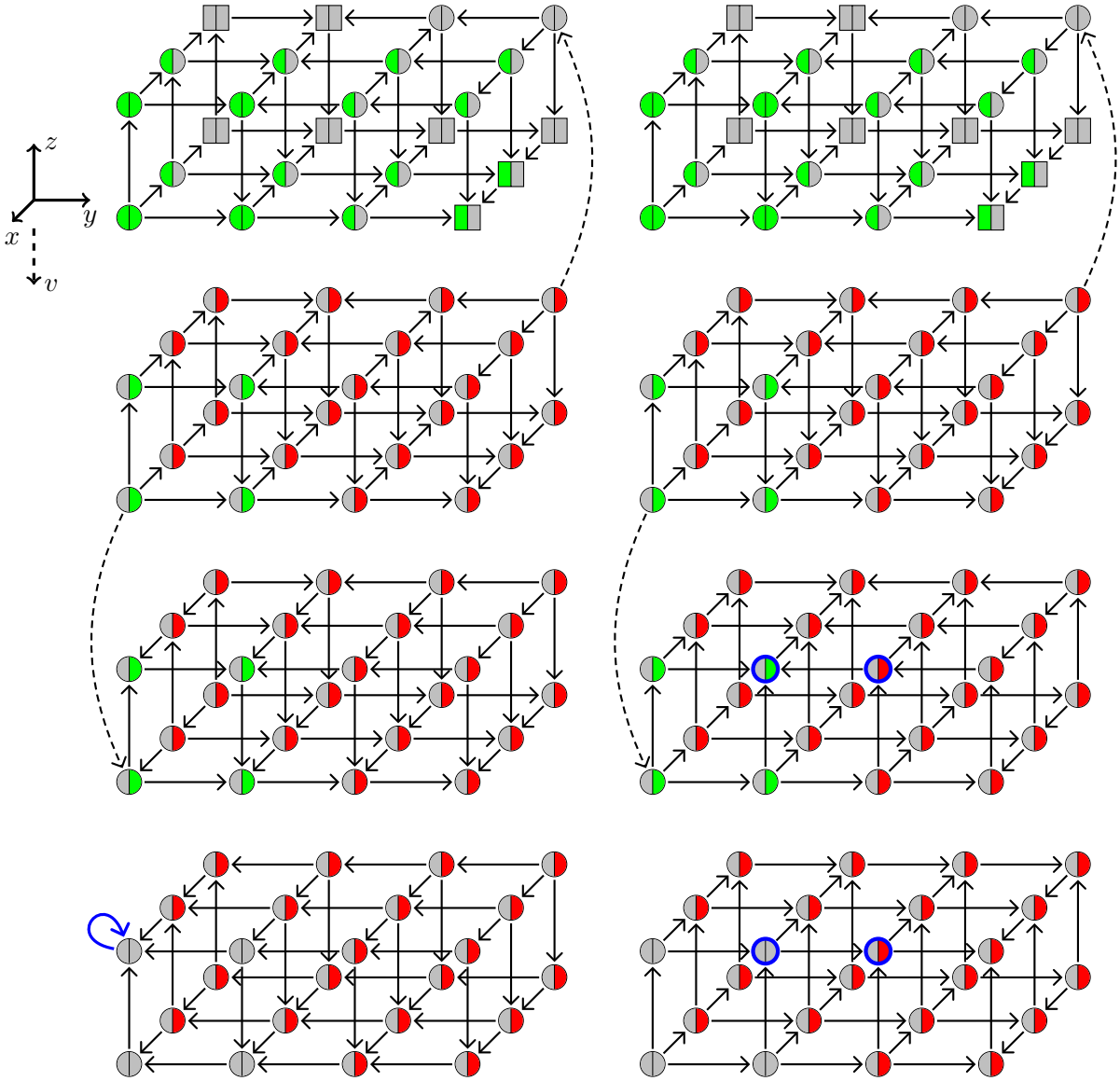

Figure 17. *Left: the complete set of all nodes represented by the top row of Figure 15, i.e., the nodes with lowest values of w. The FP is shown as a node with a blue self-loop in the lower left. The top box is a repeat of Figure 14. The same color scheme is used as in Figure 16. Example edges are shown as dotted arrows. Right: the nodes with lowest values of w from Figure 13. XC_2 is shown as the four nodes with dark blue outlines.*

REFERENCES

[1] W. Abou-Jaoude, D. Thieffry, and J. Feret, *Formal derivation of qualitative dynamical models from biochemical networks*, Biosystems, 149 (2016), pp. 70–112.

[2] R. Albert, J. J. Collins, and L. Glass, *Introduction to focus issue: Quantitative approaches to genetic networks*, Chaos, 23 (2013), 025001.

[3] U. Alon, *An Introduction to Systems Biology*, Chapman & Hall/CRC, Boca Raton, FL, 2007.

[4] Y. Artzy-Randrup, S. Fleishman, N. Ben-Tal, and L. Stone, *Comment on network motifs: Simple building blocks of complex networks and superfamilies of evolved and designed networks*, Science, 305 (2004), 1107.

[5] G. Batt, C. Belta, and R. Weiss, *Model checking genetic regulatory networks with parameter uncertainty*, in Hybrid Systems: Computation and Control, A. Bemporad, A. Bicchi, and G. Buttazzo, eds., Springer, Berlin, 2007, pp. 61–75.

[6] G. Batt, D. Ropers, H. de Jong, J. Geiselmann, R. Mateescu, M. Page, and D. Schneider, *Validation of qualitative models of genetic regulatory networks by model checking: Analysis of the nutritional stress response in escherichia coli*, Bioinformatics, 21 (2005), pp. i19–i28, https://doi.org/10.1093/bioinformatics/bti1048.

[7] G. Batt, B. Yordanov, R. Weiss, and C. Belta, *Robustness analysis and tuning of synthetic gene networks*, Bioinformatics, 23 (2007), pp. 2415–2422.

[8] C. Belta and L. Habets, *Controlling a class of nonlinear systems on rectangles*, IEEE Trans. Autom. Control, 51 (2006), pp. 1749–1759.

[9] O. Bernard and J. Gouze, *Global qualitative description of a class of nonlinear dynamical systems*, Artific. Intell., 136 (2002), pp. 29–59, https://doi.org/10.1016/S0004-3702(01)00169-2.

[10] B. Blanchet, P. Cousot, R. Cousot, J. Feret, L. Mauborgne, A. Mine, D. Monniaux, and X. Rival, *A static analyzer for large safety-critical software*, in Proceedings of the ACM SIGPLAN 2003 Conference on Programming Language Design and Implementation, R. Cytron and R. Gupta, eds., ACM, New York, 2003, pp. 196–207.

[11] D. Burkhart and J. Sage, *Cellular mechanisms of tumour suppression by the retinoblastoma gene*, Nat. Rev. Cancer, 8 (2008), pp. 671–682.

[12] M. Chaves, E. D. Sontag, and R. Albert, *Methods of robustness analysis for Boolean models of gene control networks*, IEE Proc. Systems Biol., 153 (2006), pp. 154–167, https://doi.org/10.1049/ip-syb:20050079.

[13] M. Chinnam and D. Goodrich, *RB*1*, development, and cancer*, Current Top. Dev. Biol., 94 (2011), pp. 129–169.

[14] P. Cousot, *Constructive design of a hierarchy of semantics of a transition system by abstract interpretation*, Theoret. Comput. Sci., 277 (2002), pp. 47–103.

[15] B. Cummins, T. Gedeon, S. Harker, and K. Mischaikow, *Model rejection and parameter reduction via time series*, SIAM J. Appl. Dyn. Syst., 17 (2018), pp. 1589–1616.

[16] B. Cummins, T. Gedeon, S. Harker, K. Mischaikow, and K. Mok, *Combinatorial representation of parameter space for switching systems*, SIAM J. Appl. Dyn. Syst., 15 (2016), pp. 2176–2212.

[17] H. de Jong, J. Gouze, C. Hernandez, M. Page, T. Sari, and J. Geiselmann, *Qualitative simulation of genetic regulatory networks using piecewise-linear models*, Bull. Math. Biol., 66 (2004), pp. 301–40, https://doi.org/10.1016/j.bulm.2003.08.010.

[18] R. Edwards, *Chaos in neural and gene networks with hard switching*, Differ. Equ. Dyn. Syst., 9 (2001), pp. 187–220.

[19] R. Edwards, A. Machina, G. McGregor, and P. van den Driessche, *A modelling framework for gene regulatory networks including transcription and translation*, Bull. Math. Biol., 77 (2015), pp. 953–983, https://doi.org/10.1007/s11538-015-0073-9.

[20] F. Fages and S. Soliman, *Formal cell biology in Biocham*, in Formal Methods for Computational Systems Biology, M. Bernardo, P. Degano, and G. Zavattaro, eds., Lecture Notes in Comput. Sci. 5016, Springer, Berlin, 2008, pp. 54–80.

[21] A. Faure, A. Naldi, C. Chaouiya, and D. Thieffry, *Dynamical analysis of a generic boolean model for the control of the mammalian cell cycle*, Bioinformatics, 22 (2006), pp. e124–e131.

[22] T. Gedeon, S. Harker, H. Kokubu, K. Mischaikow, and H. Oka, *Global dynamics for steep sigmoidal nonlinearities in two dimensions*, Phys. D, 339 (2017), pp. 18–38.

[23] L. Glass and S. a. Kauffman, *Co-operative components, spatial localization and oscillatory cellular dynamics*, J. Theoret. Biol., 34 (1972), pp. 219–237, https://doi.org/10.1016/0022-5193(72)90157-9.
[24] L. Glass and S. a. Kauffman, *The logical analysis of continuous, non-linear biochemical control networks*, J. Theoret. Biol., 39 (1973), pp. 103–129, https://doi.org/10.1016/0022-5193(73)90208-7.
[25] A. Gonzalez, A. Naldi, L. Sanchez, D. Thieffry, and C. Chaouiya, *GINSIM: A software suite for the qualitative modelling, simulation, and analysis of regulatory networks*, BioSystems, 84 (2006), pp. 91–100.
[26] Z. Huttinga, B. Cummins, T. Gedeon, and K. Mischaikow, *Global dynamics for switching systems and their extensions by linear differential equations*, Phys. D, 367 (2018), pp. 19–37, https://doi.org/10.1016/j.physd.2017.11.003.
[27] P. J. Ingram, M. Stumpf, and J. Stark, *Network motifs: Structure does not determine function*, BMC Genomics, 7 (2006), 108.
[28] L. Ironi, L. Panzeri, E. Plahte, and V. Simoncini, *Dynamics of actively regulated gene networks*, Phys. D, 240 (2011), pp. 779–794, https://doi.org/10.1016/j.physd.2010.12.010.
[29] G. Karlebach and R. Shamir, *Modelling and analysis of gene regulatory networks*, Nature, 9 (2008), pp. 770–780.
[30] W. Ma, A. Trusina, H. El-Samad, W. A. Lim, and C. Tang, *Defining network topologies that can achieve biochemical adaptation*, Cell, 138 (2009), pp. 760–773.
[31] A. Manning and N. Dyson, *RB: Mitotic implications of a tumour suppressor*, Nat. Rev. Cancer, 12 (2012), pp. 220–226.
[32] S. C. Shah NA, *Robust network topologies for generating switch-like cellular responses*, PLoS Comput. Biol., 7 (2011), e1002085.
[33] S. N. Steinway, M. B. Biggs, T. P. Loughran, J. A. Papin, and R. Albert, *Inference of network dynamics and metabolic interactions in the gut microbiome*, PLOS Comput. Biol., 11 (2015), e1004338.
[34] R. Thomas, *Boolean formalization of genetic control circuits*, J. Theoret. Biol., 42 (1973), pp. 563–585, https://doi.org/10.1016/0022-5193(73)90247-6.
[35] R. Thomas, *Regulatory networks seen as asynchronous automata: A logical description*, J. Theoret. Biol., 153 (1991), pp. 1–23, https://doi.org/10.1016/S0022-5193(05)80350-9.
[36] R. Thomas, D. Thieffry, and M. Kaufman, *Dynamical behaviour of biological regulatory networks*-I. *Biological role of feedback loops and practical use of the concept of the loop-characteristic state*, Bull. Math. Biol., 57 (1995), pp. 247–276.
[37] L. Tournier and M. Chaves, *Uncovering operational interactions in genetic networks using asynchronous boolean dynamics*, J. Theoret. Biol., 260 (2009), pp. 196–209, https://doi.org/10.1016/j.jtbi.2009.06.006.